# Total Life Casting Process Development and Effect of Porosity on Performance of Steel Castings

Richard Hardin, Research Engineer
Christoph Beckermann, Professor

Solidification Laboratory
Department of Mechanical and Industrial Engineering
The University of Iowa
Iowa City, Iowa

Society of Automotive Engineers Fatigue, Design, and Evaluation Committee Meeting
Spring 2021

Held Virtually
May 11, 2021

# Integrated Process and Mechanical Design of Castings

- Discontinuities from casting process and their effects on performance are not considered in casting design.

Inclusions

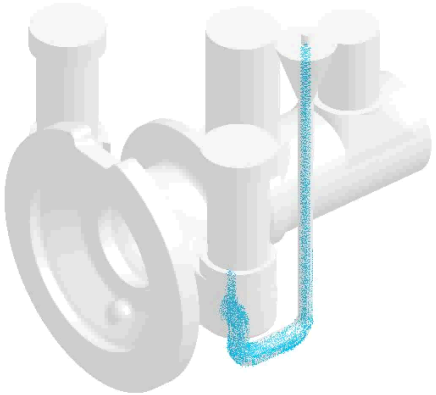

Cracks/Hot Tears

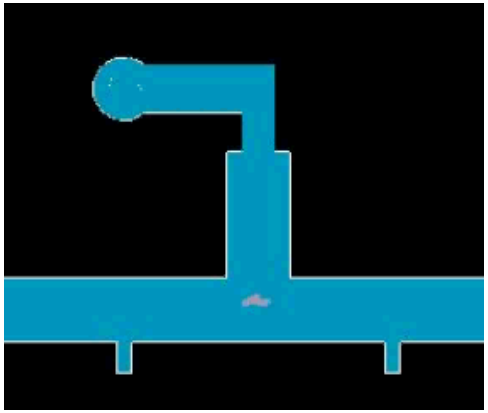

Porosity

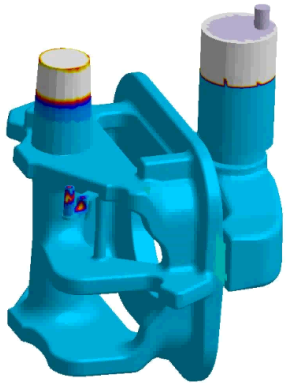

- Combine computer modeling of casting process and stress analysis to predict the effects of discontinuities on casting performance: elastic, plastic, fatigue and failure.

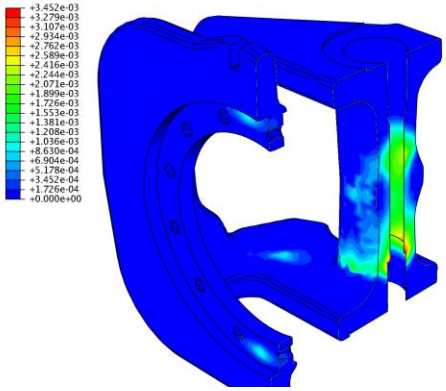

Porosity Fraction

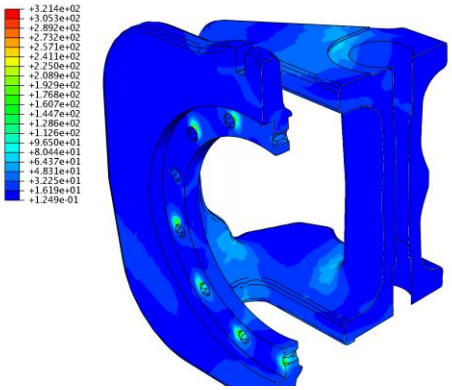

Von Mises Stress (MPa)

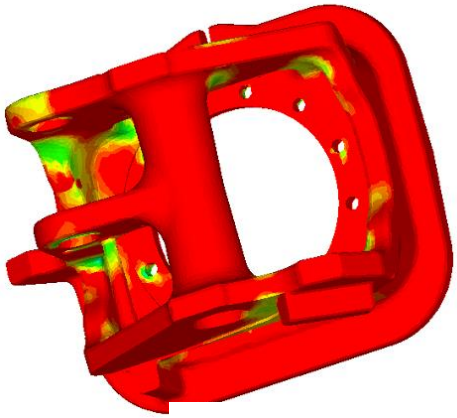

Fatigue Life

# Benefits of Integrating Casting Process and Design

- Predicting casting performance
  - reduces trial and error engineering
  - fewer failures in the field
- Castings designed for performance
  - can be lighter
  - produced faster
- Improving inspection requirements (NDE) and relating NDE to mechanical performance will improve reliability
- Reduce time and costly test programs required to validate casting designs

- Framework for predicting fatigue life will be applied to a cast version of the SAE Total Life Specimen.

# SAE Total Life Specimen

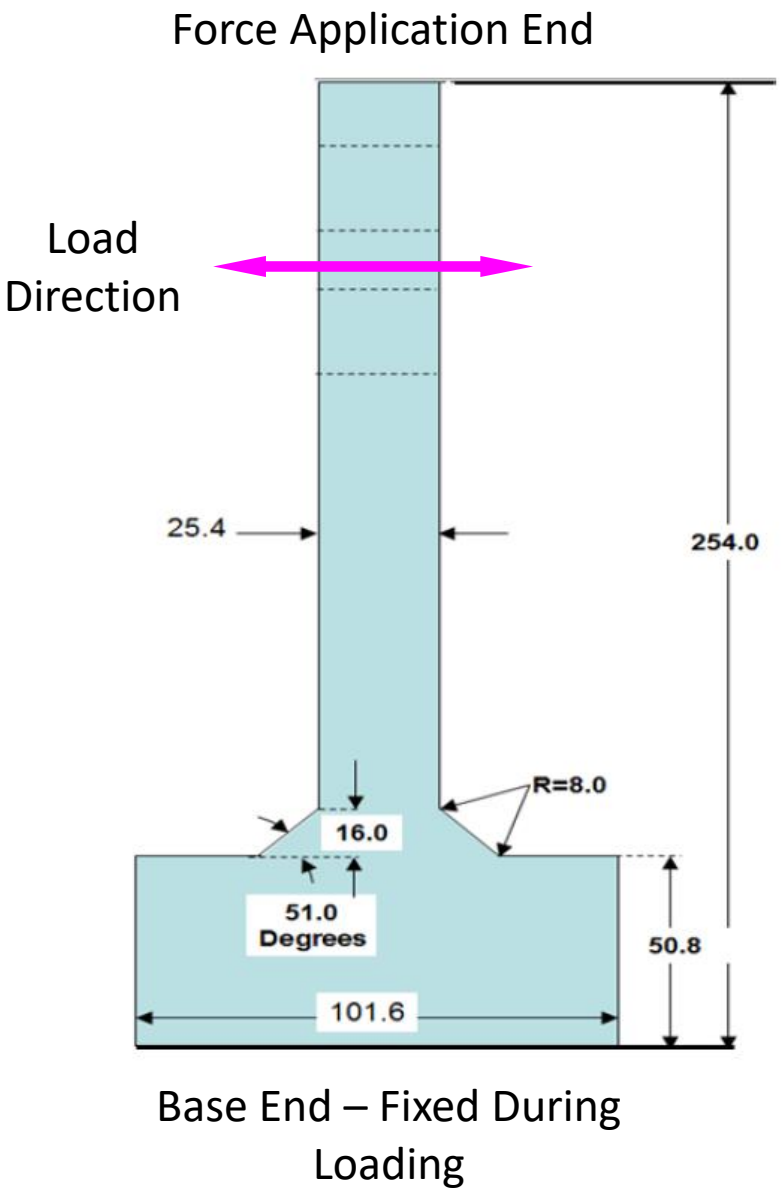


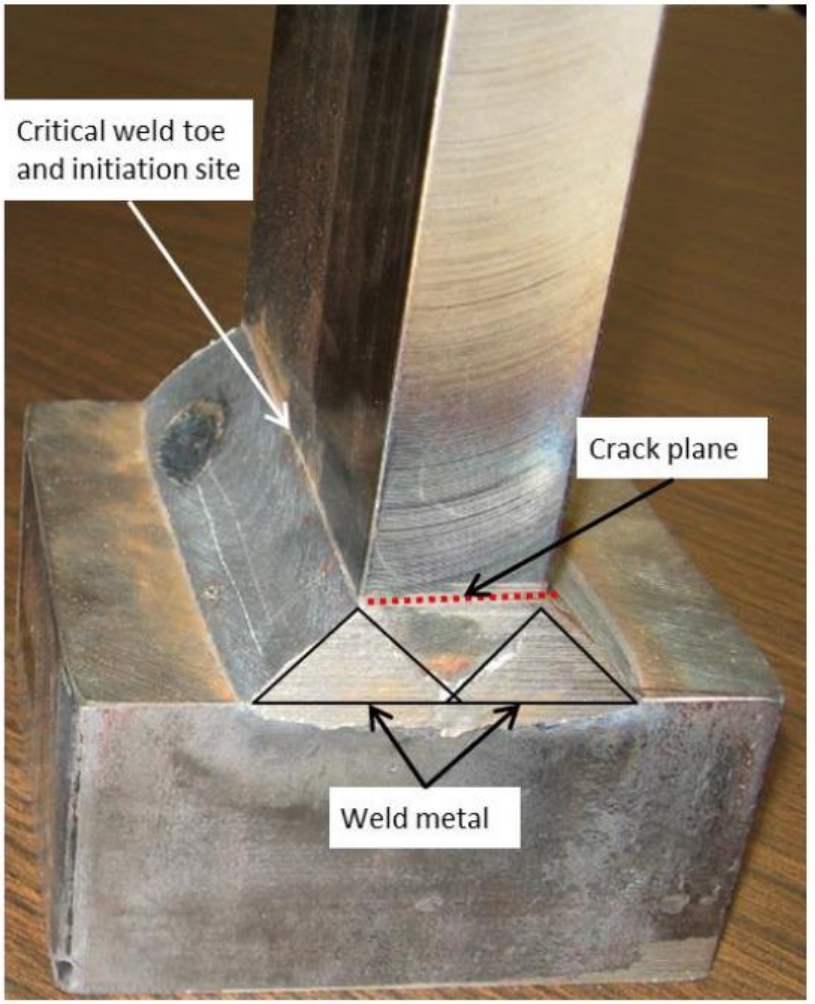

# Casting Specimen Dimensions

- Bracket model, no shrinkage allowance applied

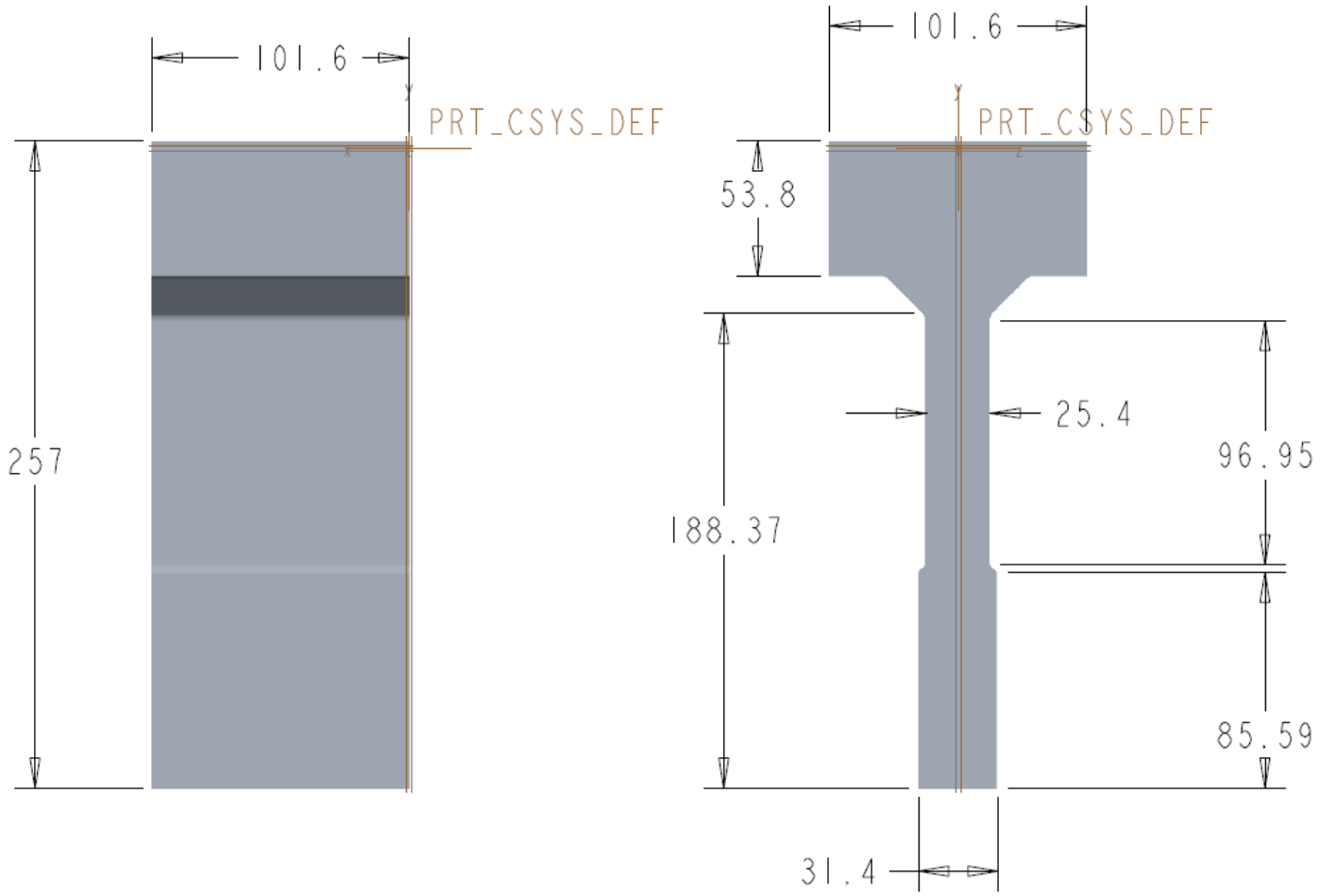

# Casting Specimen Dimensions with 2.1% Shrink Rule

- Bracket model, 2.1% shrinkage allowance applied

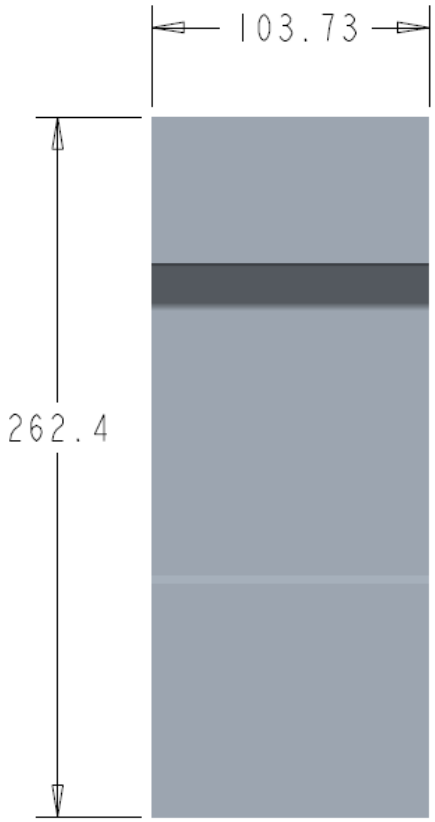


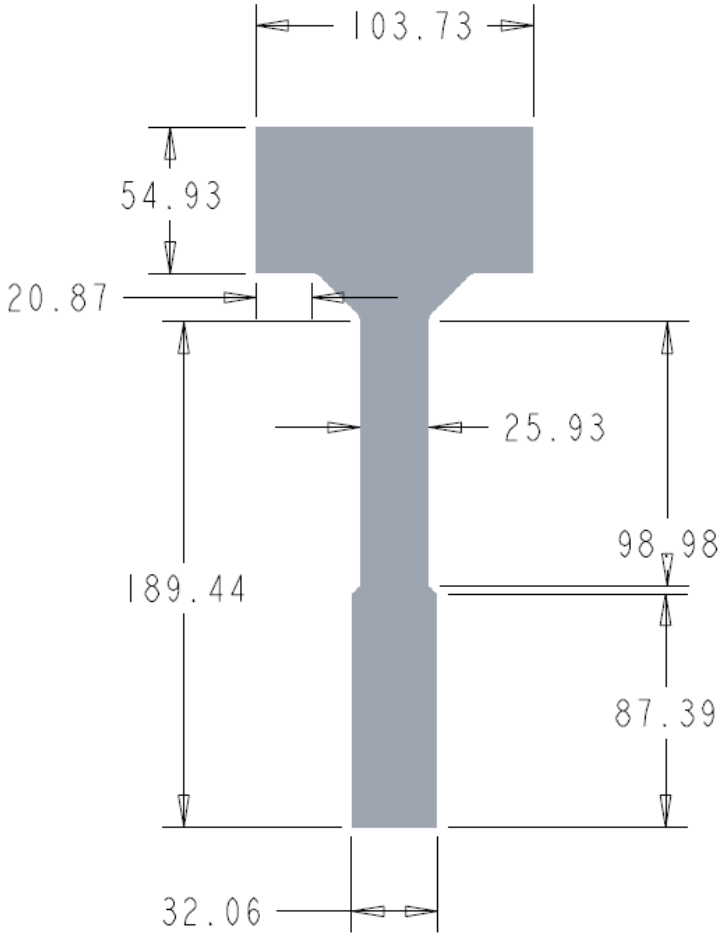

# SAE Total Life Casting Specimens

Cast Specimen –
Weldment Type

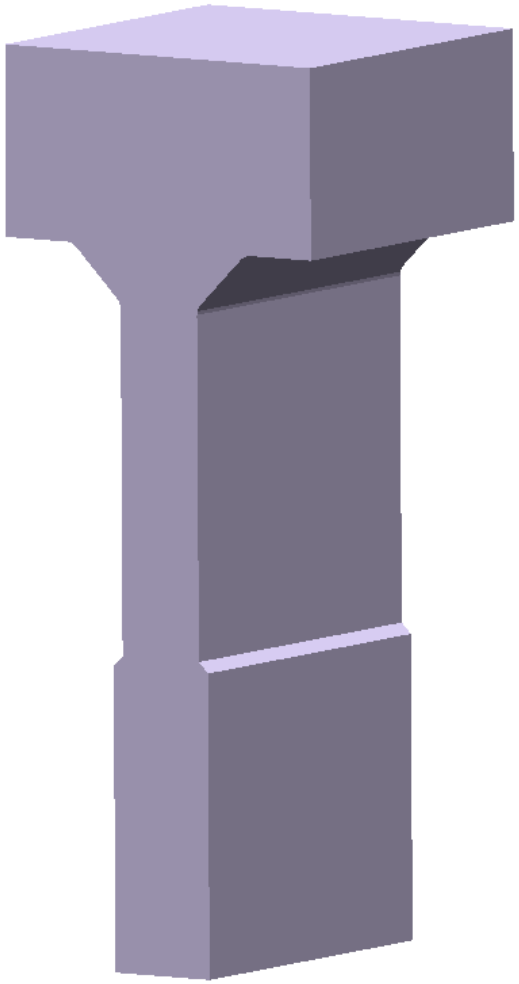

Cast Specimen –
Casting Type

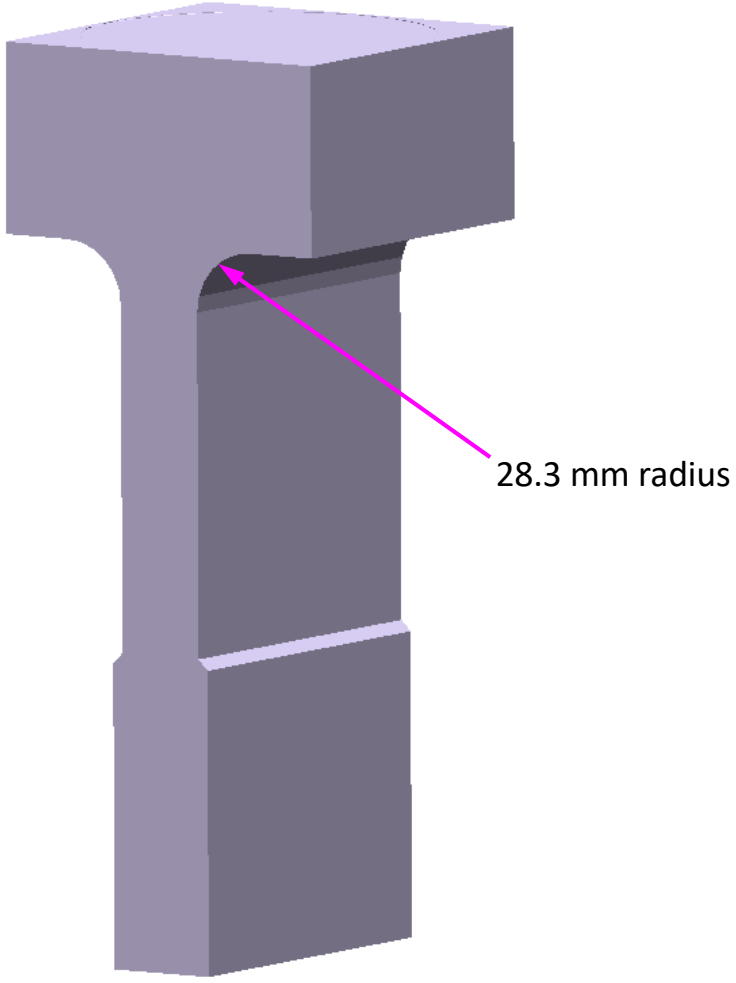

# Development of Process Rigging and Pouring Configuration

- Sequential pouring using a basin. Pour castings quicker and hotter.

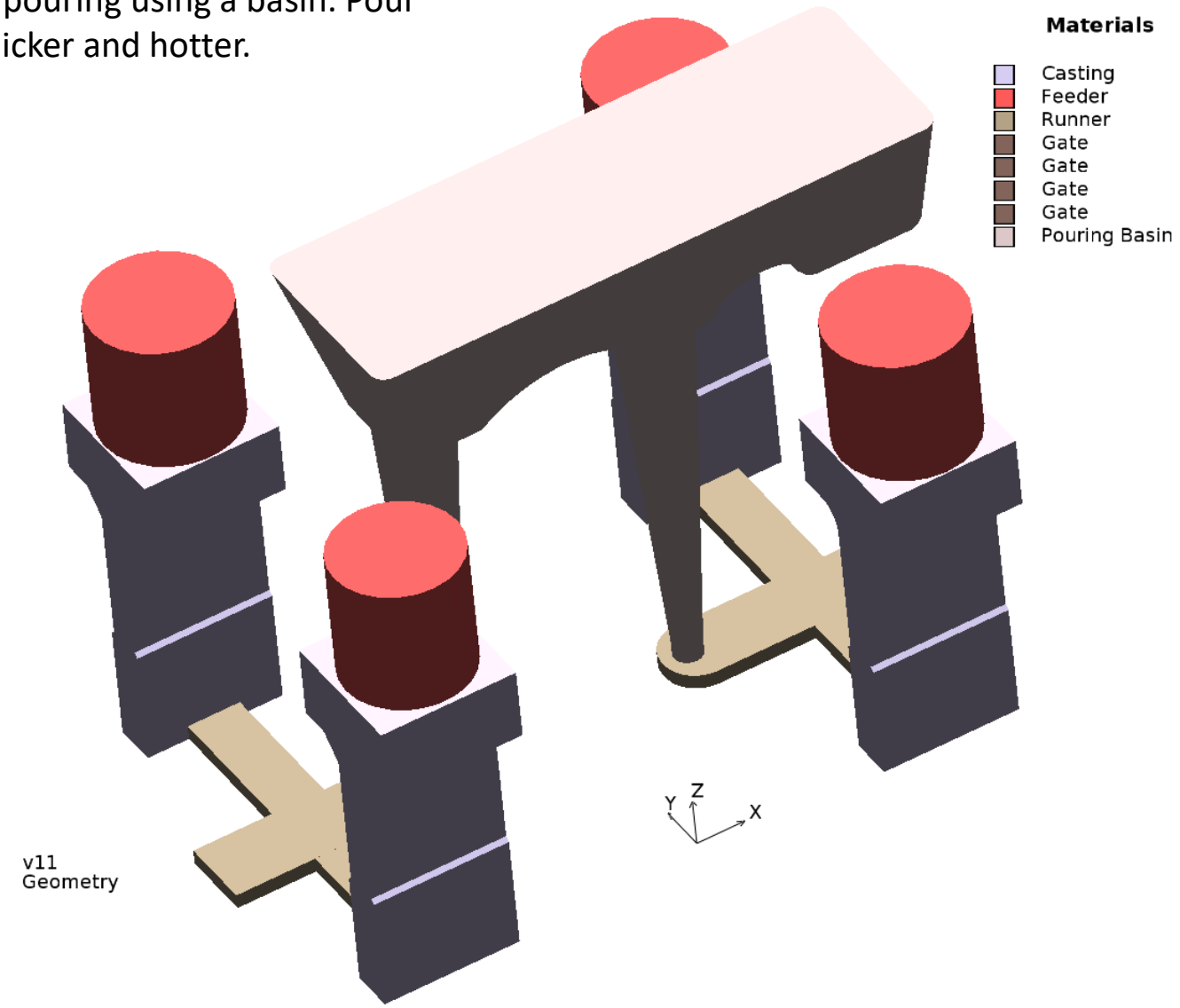


- Two brackets of weldment-type, and two of casting-type per mold poured.

# Simulation Results - Temperature During Filling

- Advance slides in presentation mode to view animation.

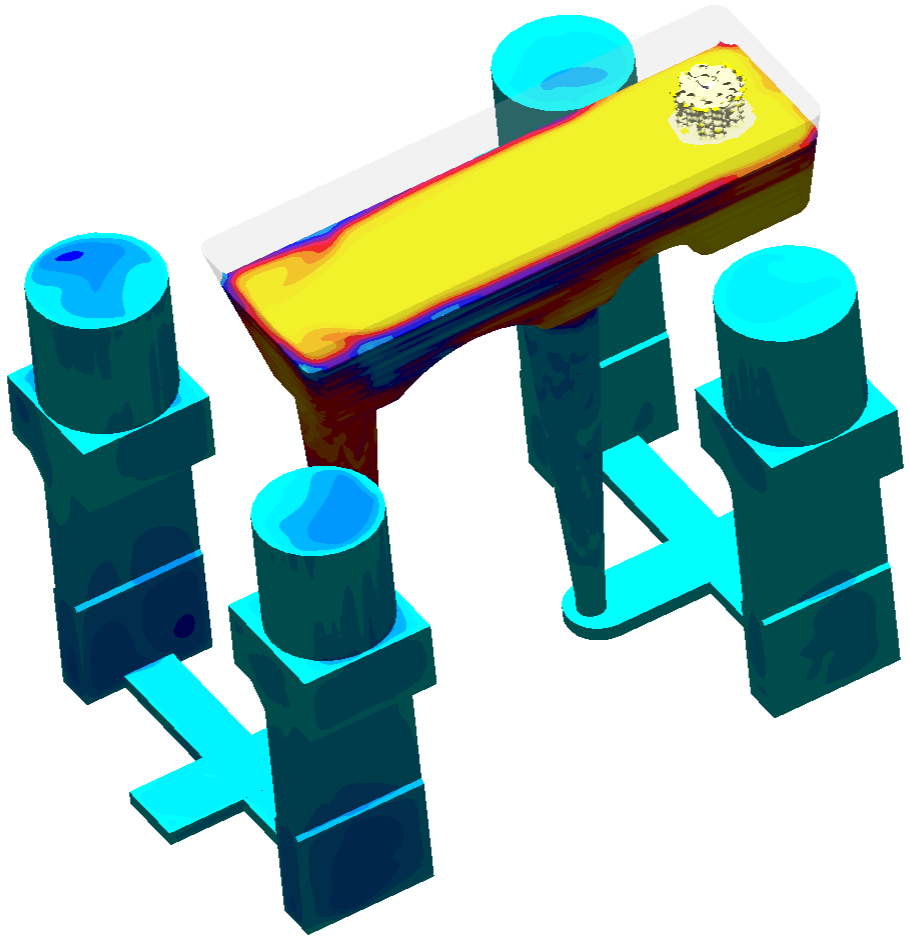

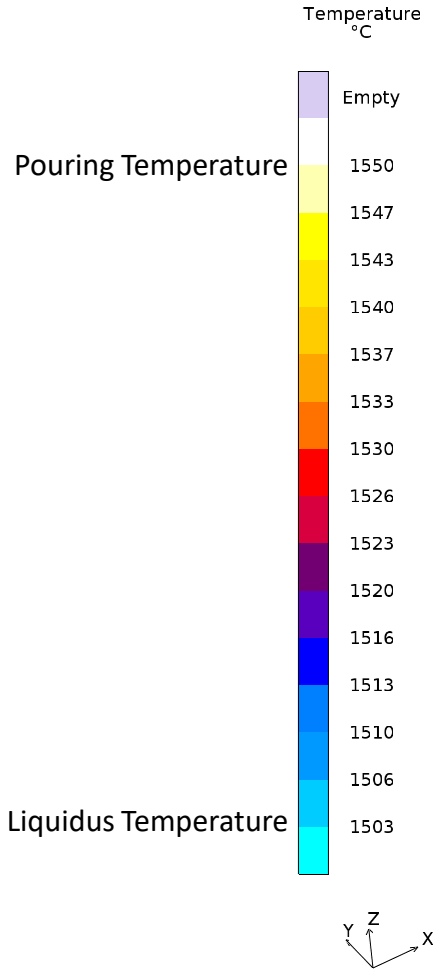


v11
Pouring, Temperature
42.721s, 87.86 %
X-Ray: on

# Simulation Results - Porosity for Weldment-Type Castings

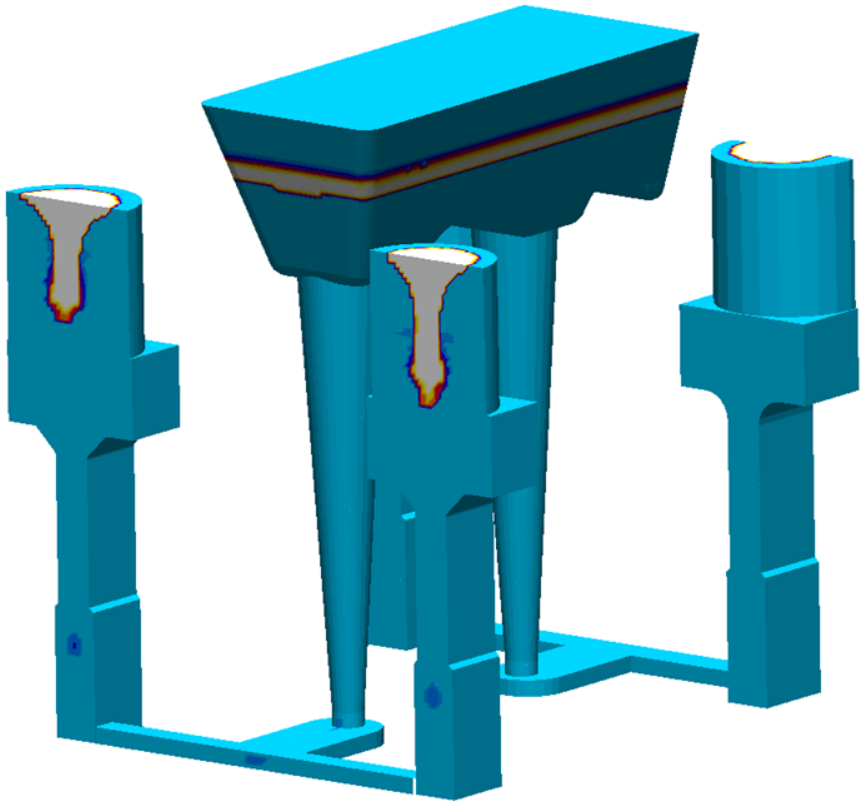

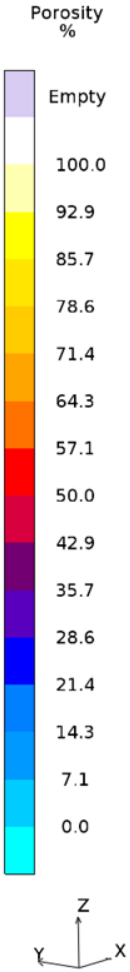





v11
Solidification & Cooling, Porosity
21min 39.1s, 100.00 %
X-Ray: off

# Simulation Results - Porosity for Casting Type Specimens

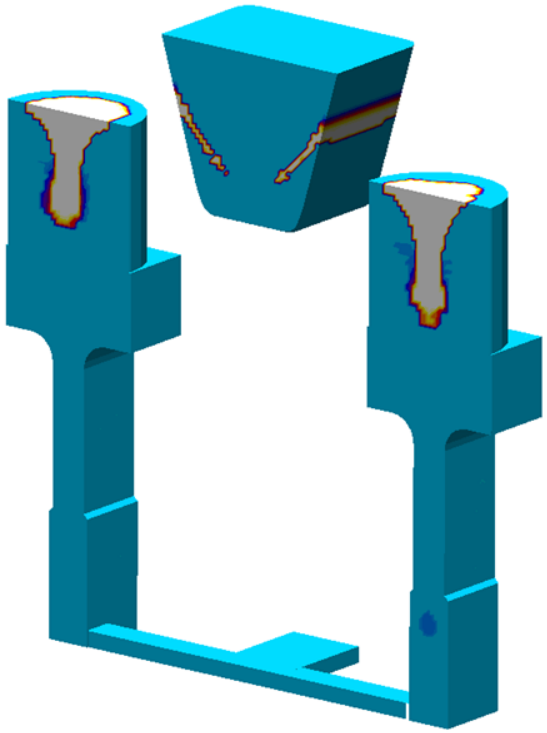

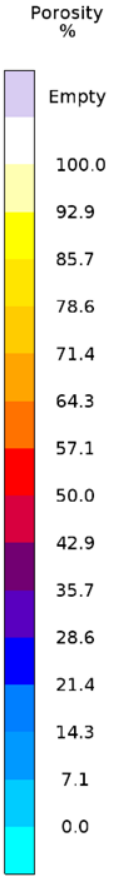


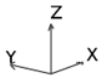


v11
Solidification & Cooling, Porosity
21min 39.1s, 100.00 %
X-Ray: off

MAGMA

# Example Sand Mold Model for 3D Printing

- View in presentation mode and advance to see slices.

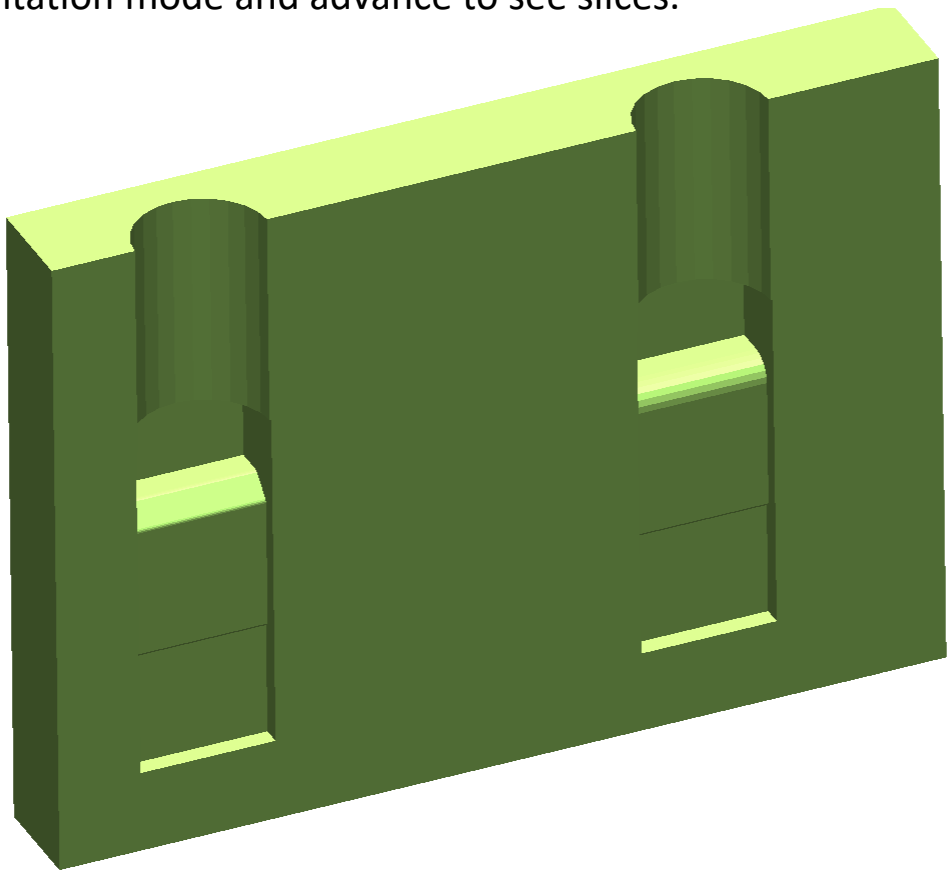

# Final Rigging for Cast Specimens – Steel without Porosity

- Two casting-type, one weldment-type and one with printed surface porosity per mold poured

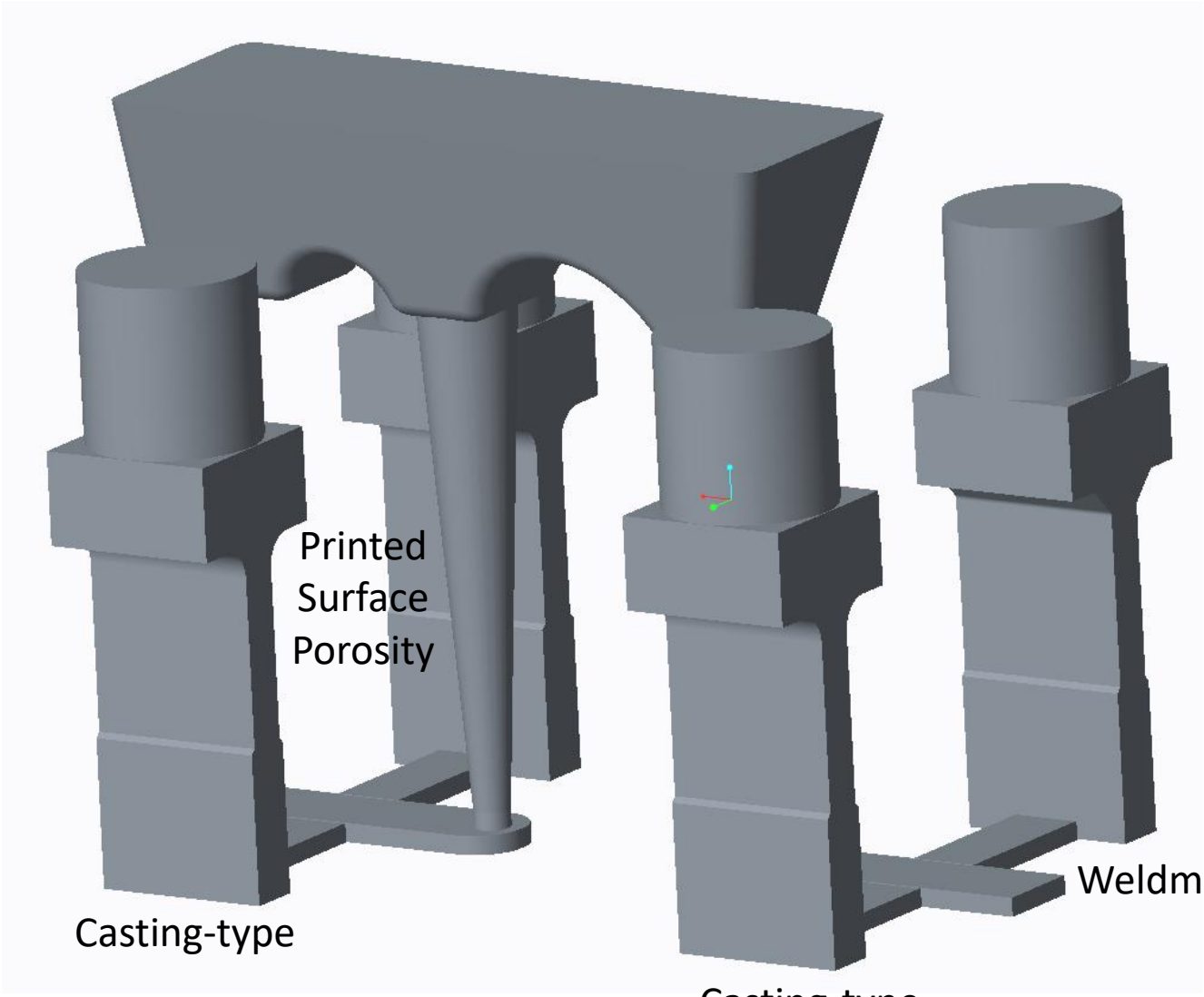

# Final Rigging for Cast Specimens – Steel without Porosity

- Two casting-type, one weldment-type and one with printed surface porosity per mold poured

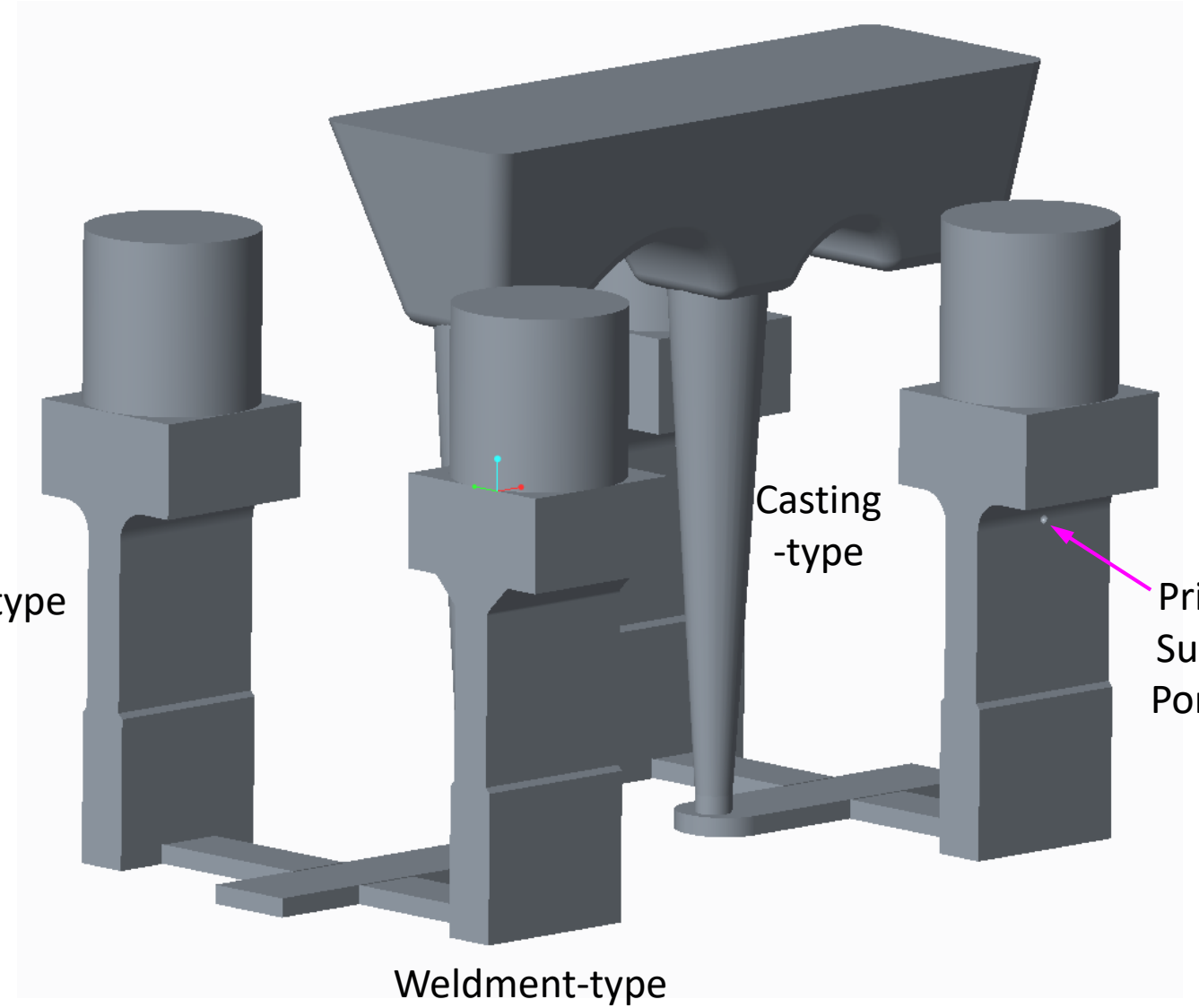

# Development of Process Rigging – Specimens with Porosity

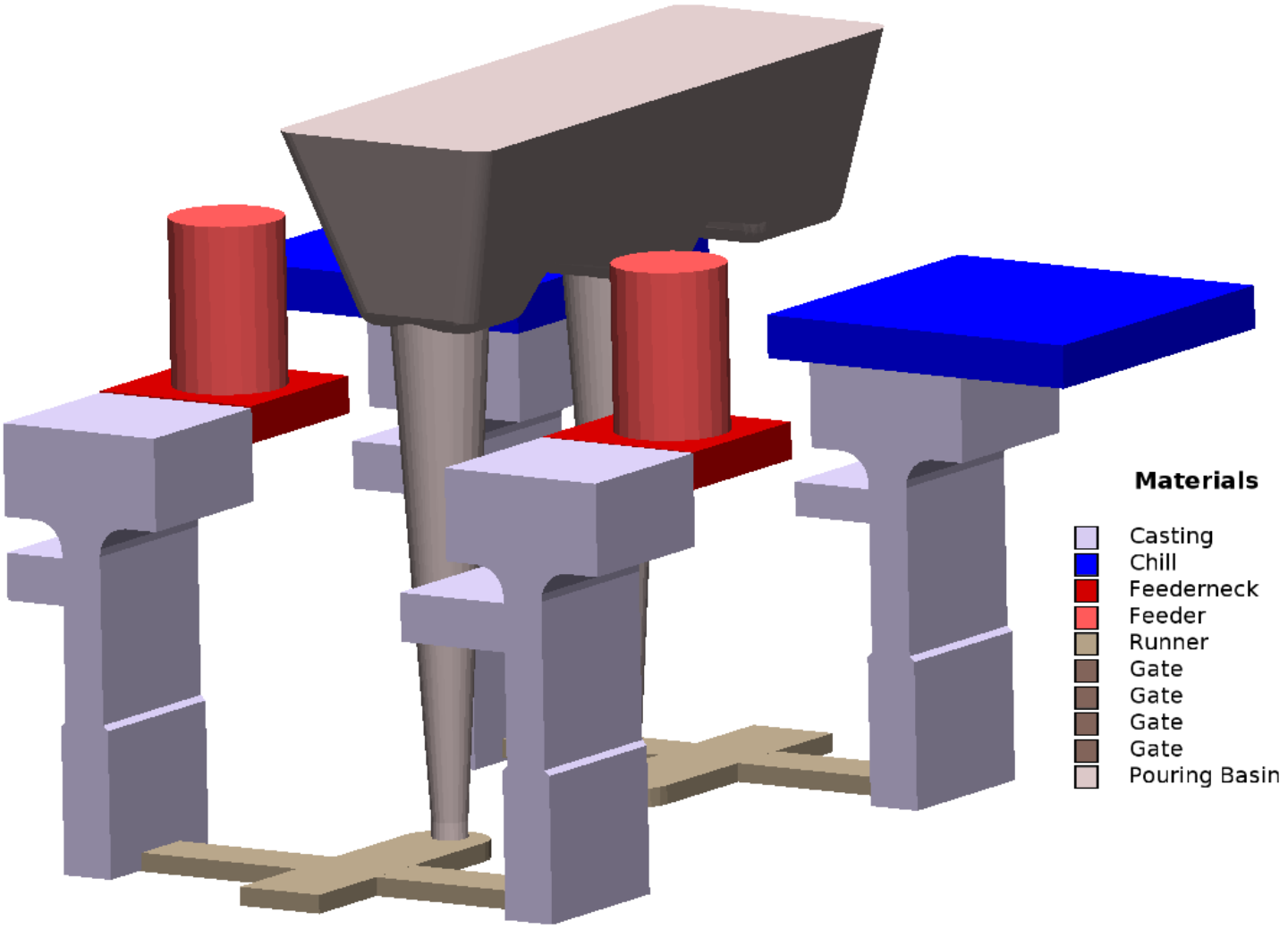

# Development of Process Rigging – Specimens with Porosity

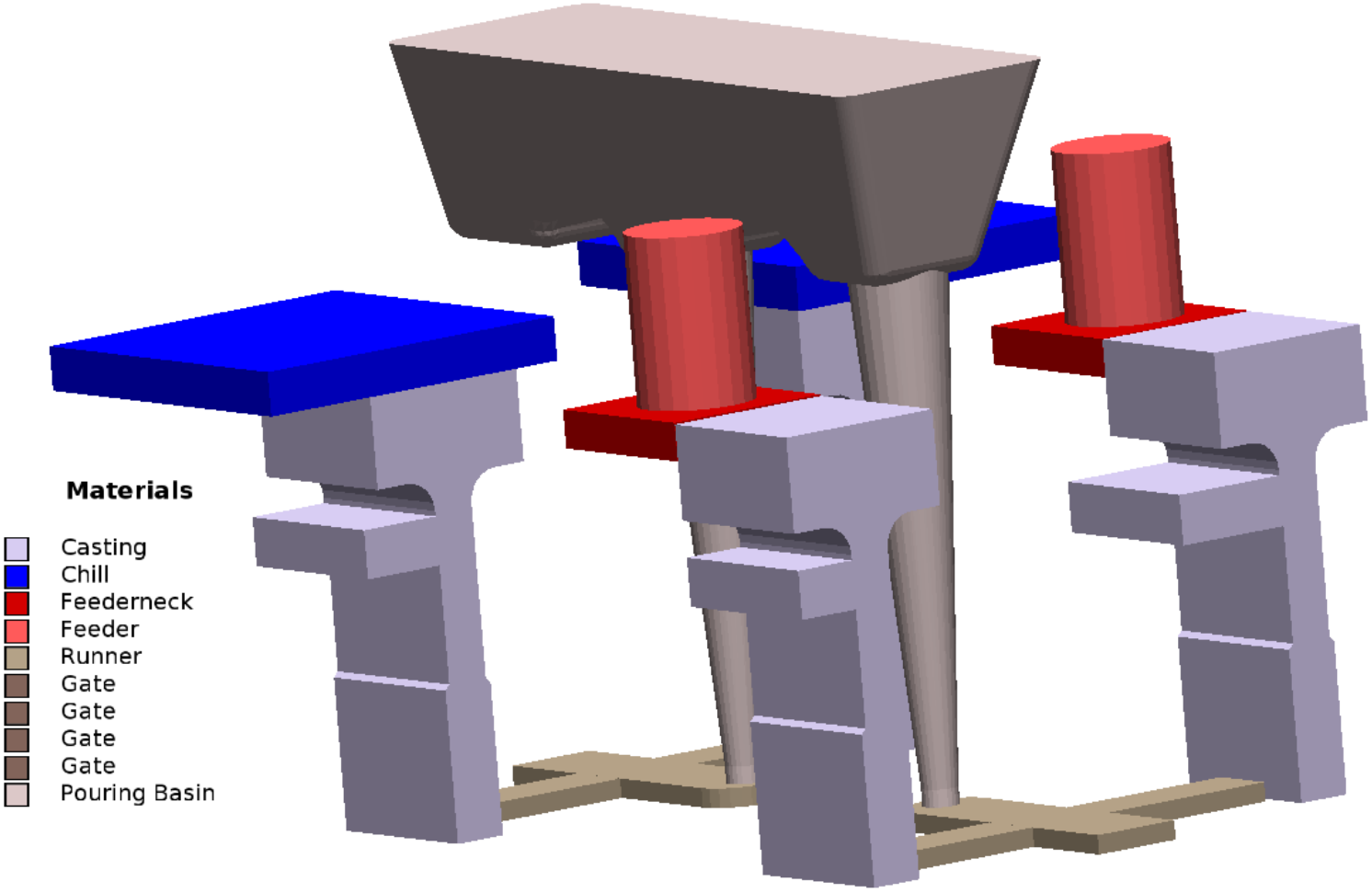

# Simulation Results – Solidification Progression and Porosity

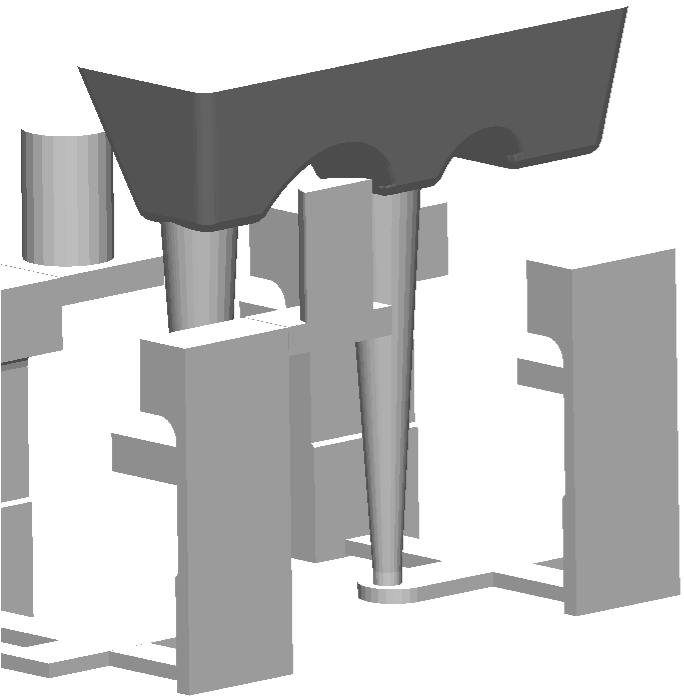

v24
Solidification & Cooling, Fraction Solid
14min 20.8s, 100.00 %
X-Ray: off

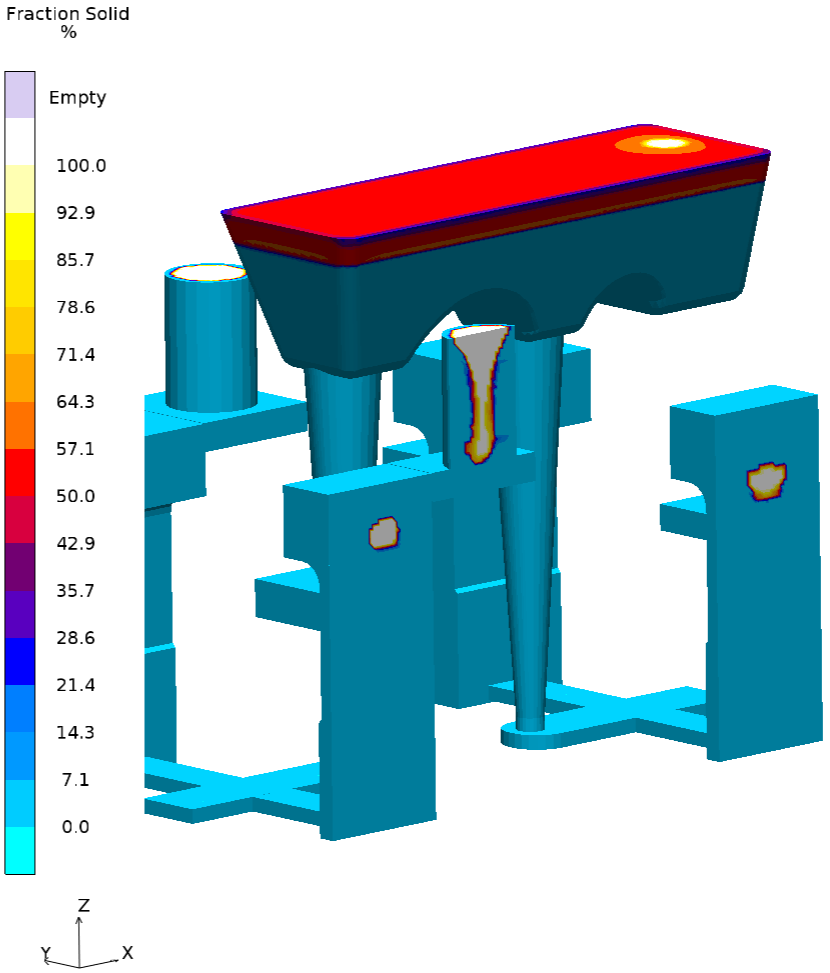


v24
Solidification & Cooling, Porosity
14min 20.8s, 100.00 %
X-Ray: off

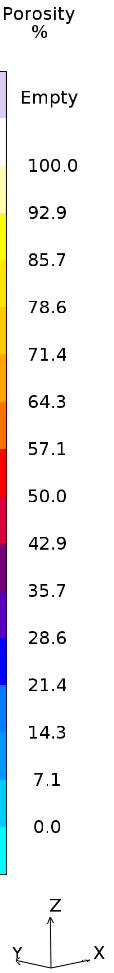

# Simulation Results - Porosity Casting with Porosity

- Specimens with porosity discontinuities will be used in study to gage accuracy of method to prediction casting performance in their presence.

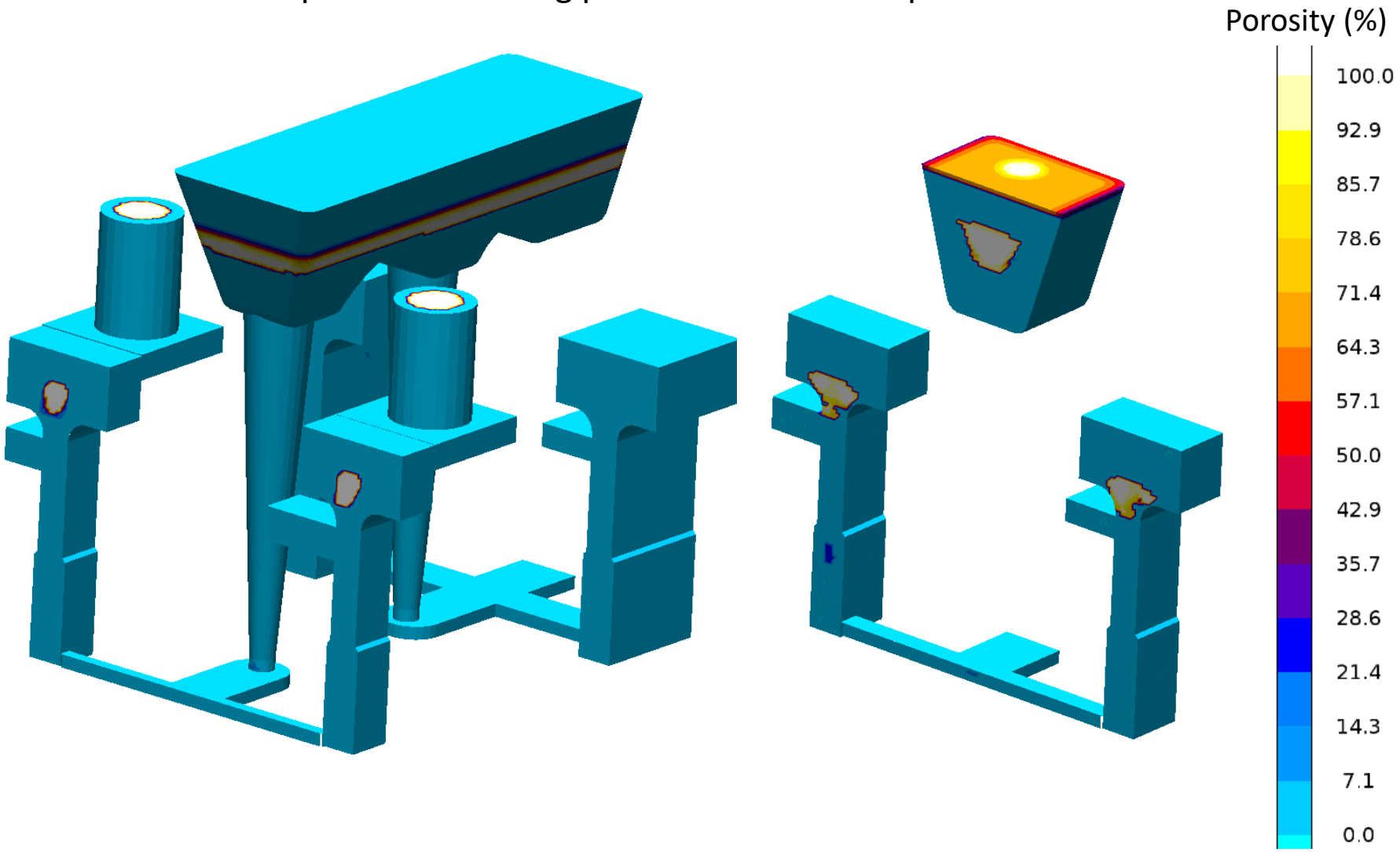

# Effect of Porosity on Stiffness and Fatigue

- A loss of stiffness results in Stress Redistribution

Stress Distributions in Suspension Part With and Without Porosity

Porosity from Casting Simulation

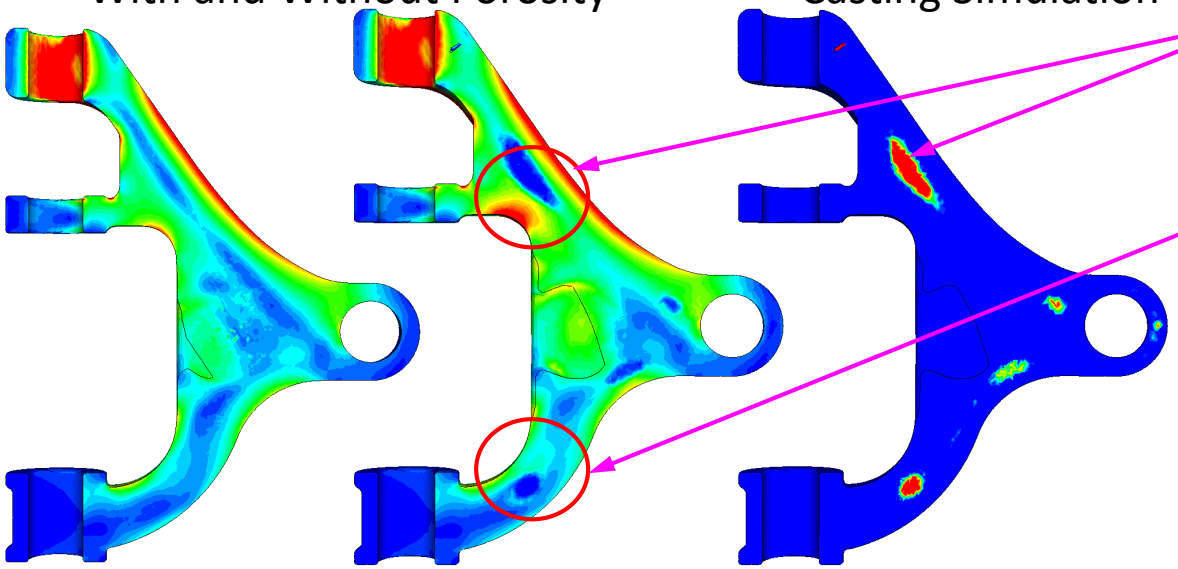

Red = High Stress or High Porosity Region.

Here the porosity causes little increase in stress.

Without porosity

With Porosity

- Stress riser or concentration site for fatigue crack initiation
  - SEM image of near-surface micropore, initiation site for fatigue fracture, approximately 200 µm in diameter.

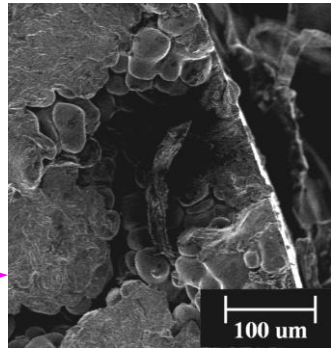

# Effect of Porosity on Elastic Behavior and Fatigue: Porosity Measurements and Reconstruction from Radiographs

Test Specimen Castings Produced with Porosity in Gage Section – Designed using Simulation

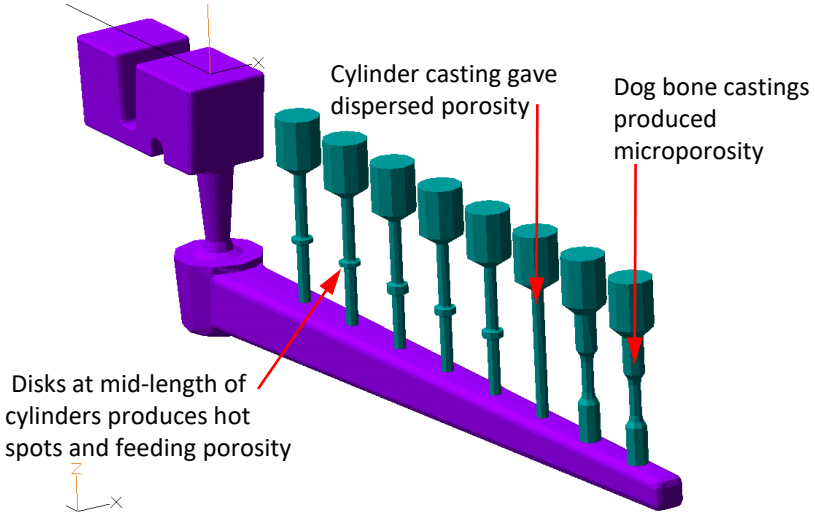


Test Specimens Machined with Porosity Positioned in Gage Section

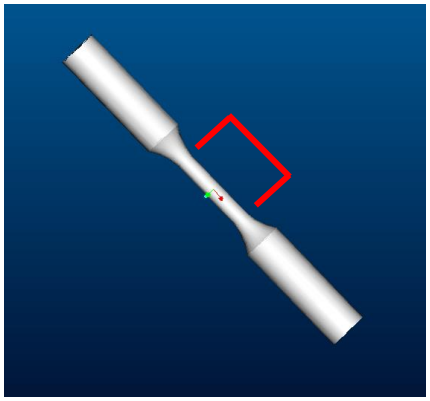

Radiography of Specimens from Orthogonal Views

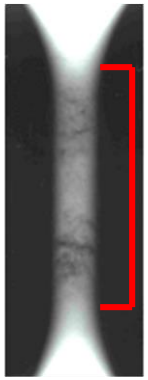

Algebraic Tomographic Reconstruction of Porosity in Gage Section Performed to Map it to Nodes in ABAQUS FEA Stress Model

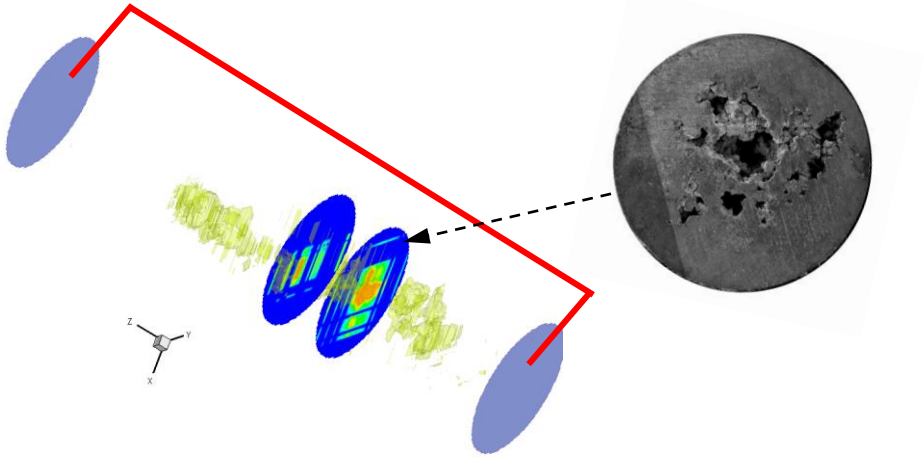

# Test Specimens with Porosity

- Generated wide range of porosity levels, sizes and distributions

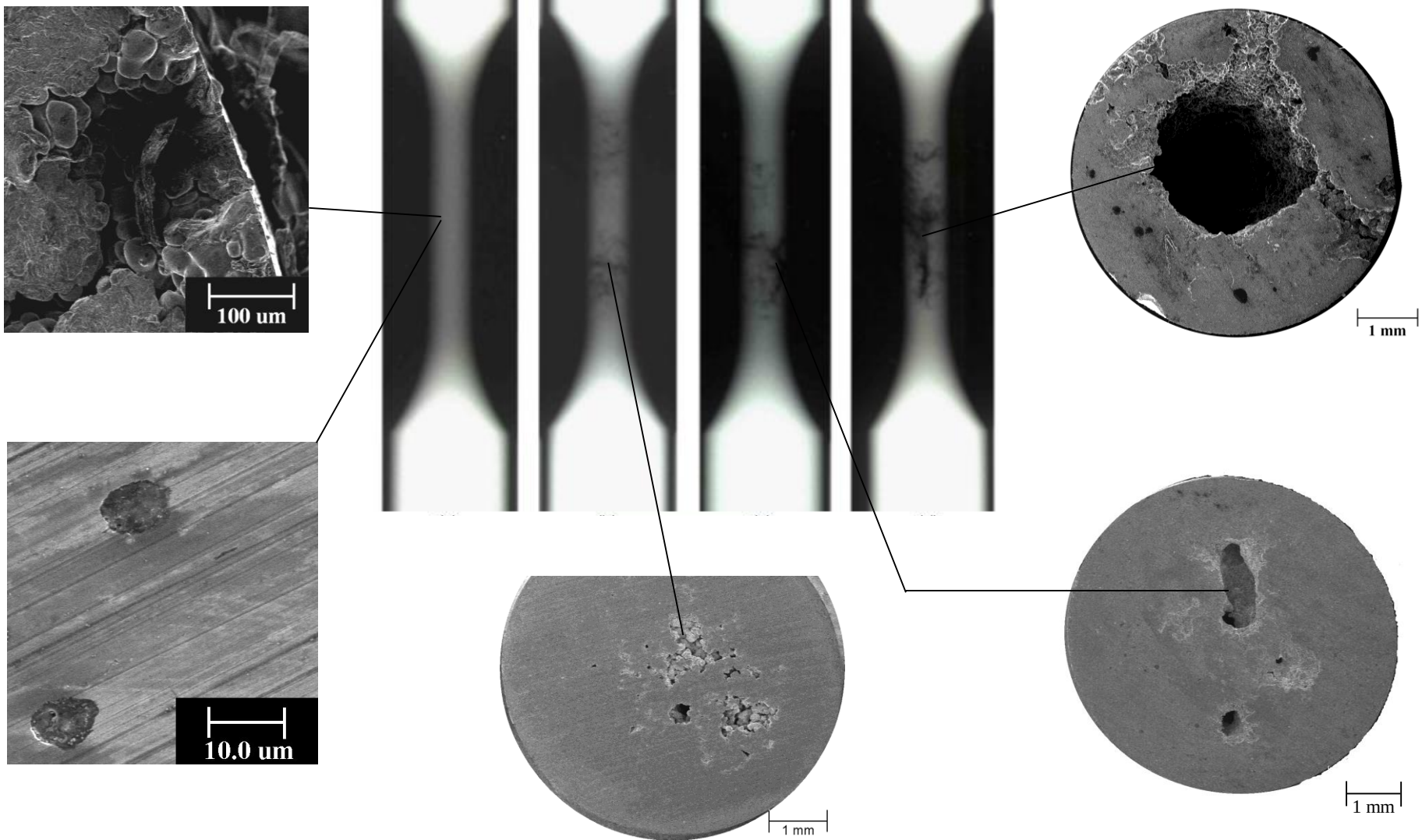

# Effect of Microporosity on Fatigue

- Micropores of ≈10 μm diam on surface of a specimen.

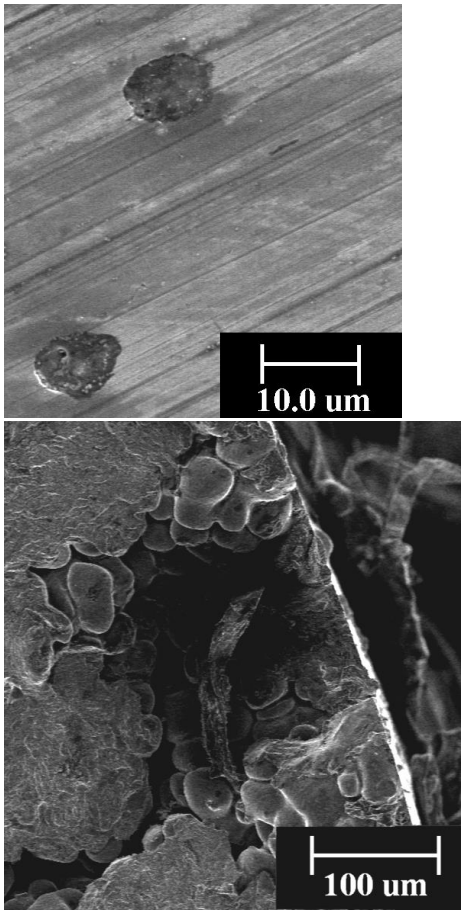


- Near-surface micropore ≈ 200 μm diam on fracture surface.

- Strain-life curve for 8630 steel with microporosity specimen data, and strain-life calculations using 10, 20, 100 and 200 μm diameter spherical Neuber notches.

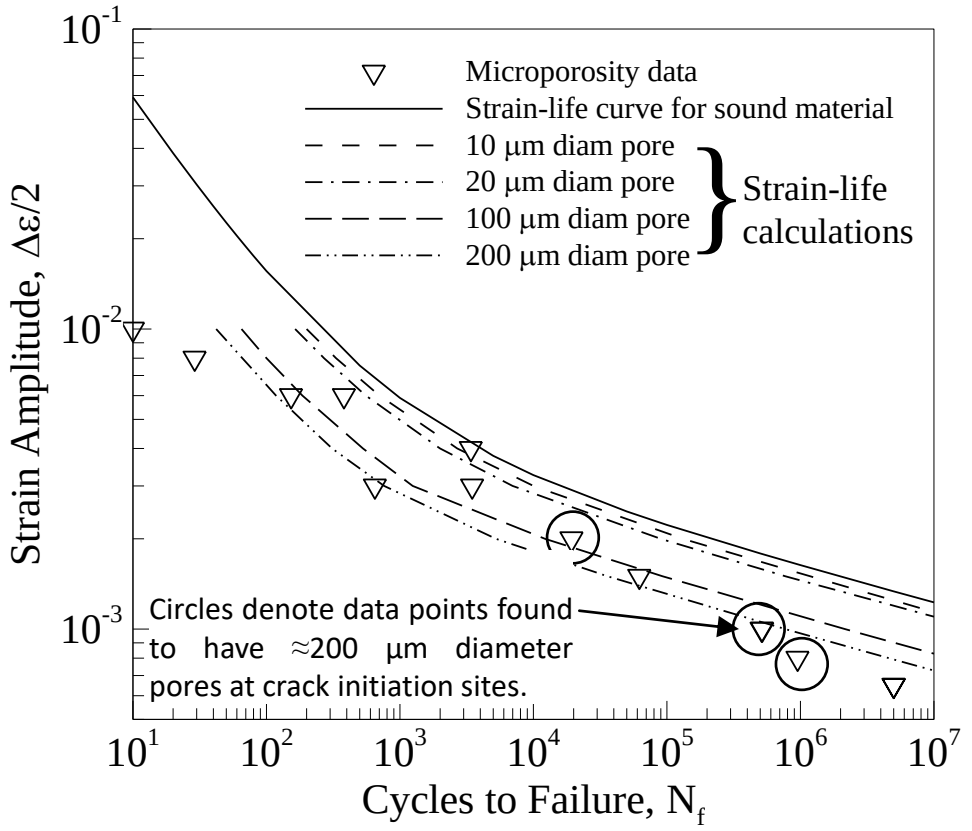

# Microporosity Results: Predicted vs. Experimental Fatigue Life

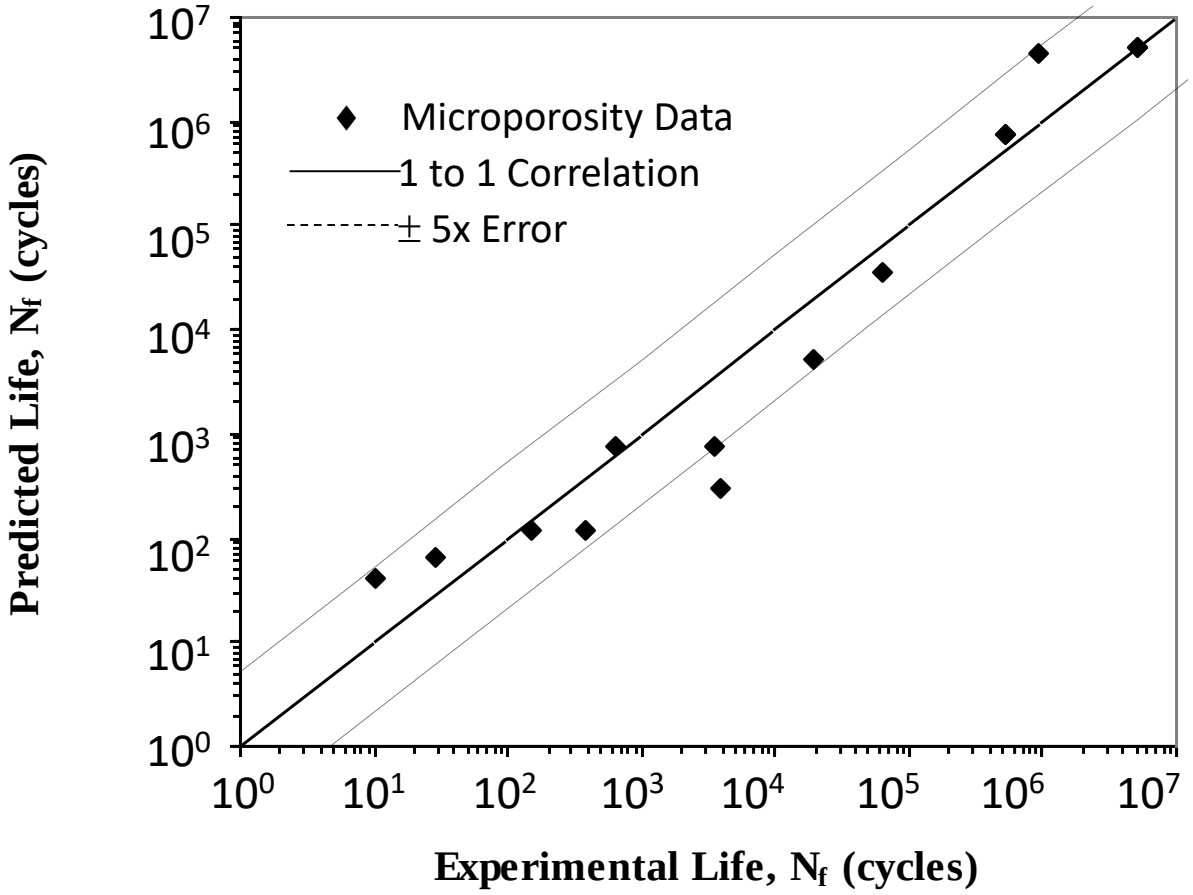


- Predicted life calculated using sound material properties with a 200 µm diameter spherical notch

# Effect of Porosity Shape and Size

- Different *E* for same average porosity of 30% depending on shape!

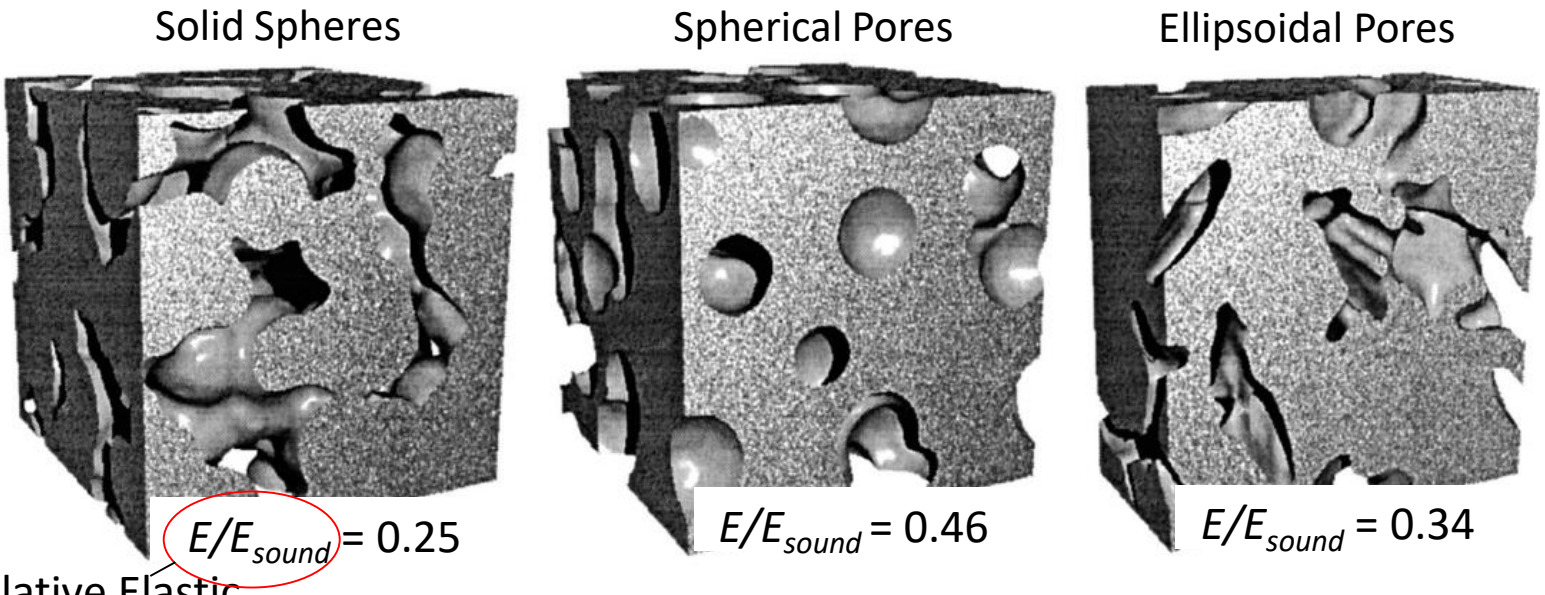


- With increasing porosity, solid ceases to be interconnected and $E = 0$.

- This occurs at a critical porosity level which can vary depending on shape.

From: Roberts and Garboczi, *J. Am. Ceram. Soc.*, (2000).

# Effect of Porosity Shape and Size

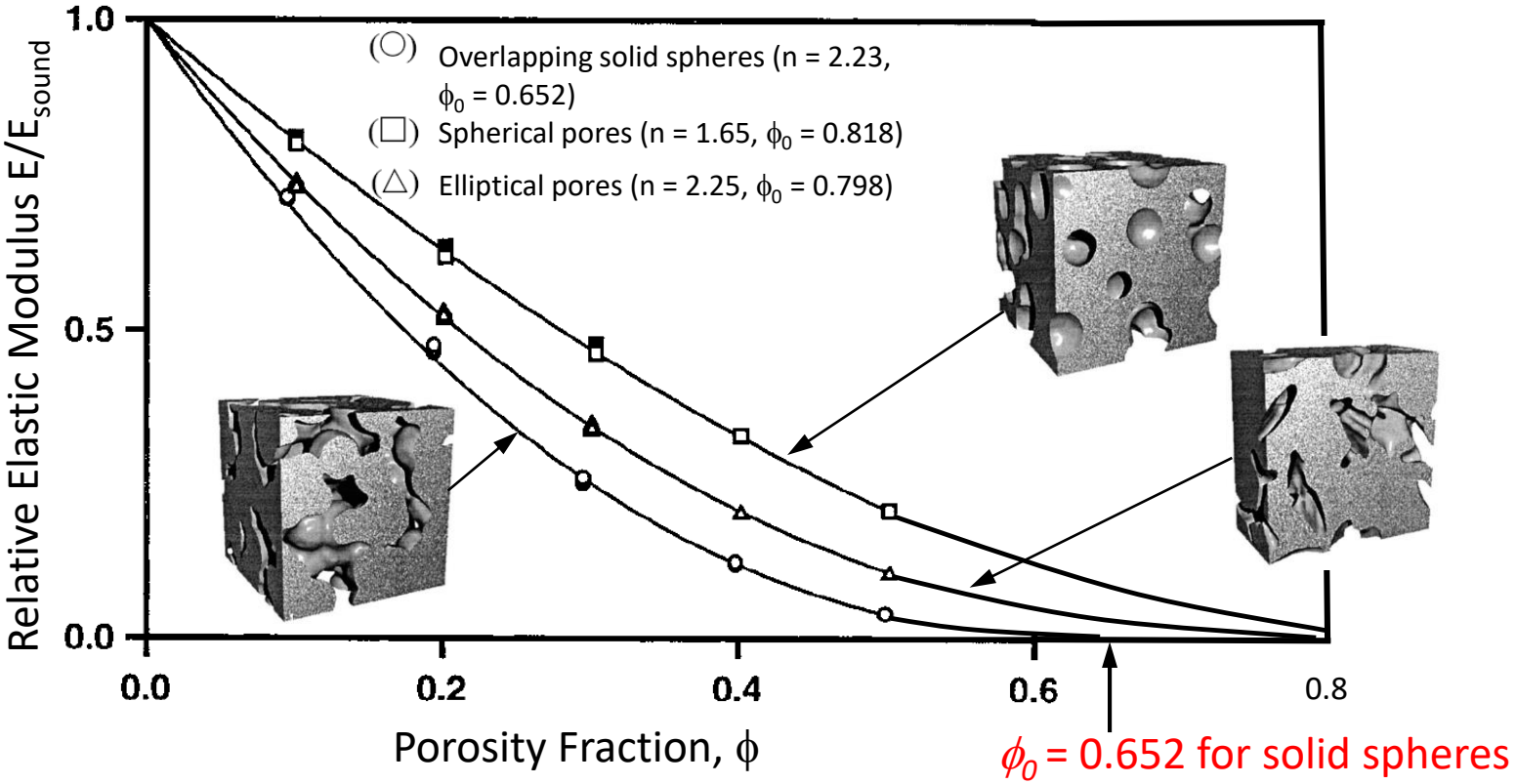


- Follows power law relation

$$E(\phi) = E_{sound}\left(1-\frac{\phi}{\phi_0}\right)^n$$

where $n$ is the power law exponent and $\phi_0$ is critical pore fraction where $E = 0$.

From: Roberts and Garboczi, *J. Am. Ceram. Soc.*, (2000).

# Effect of Porosity Distribution

Test Specimens with Equal Average Porosity in Gage Section

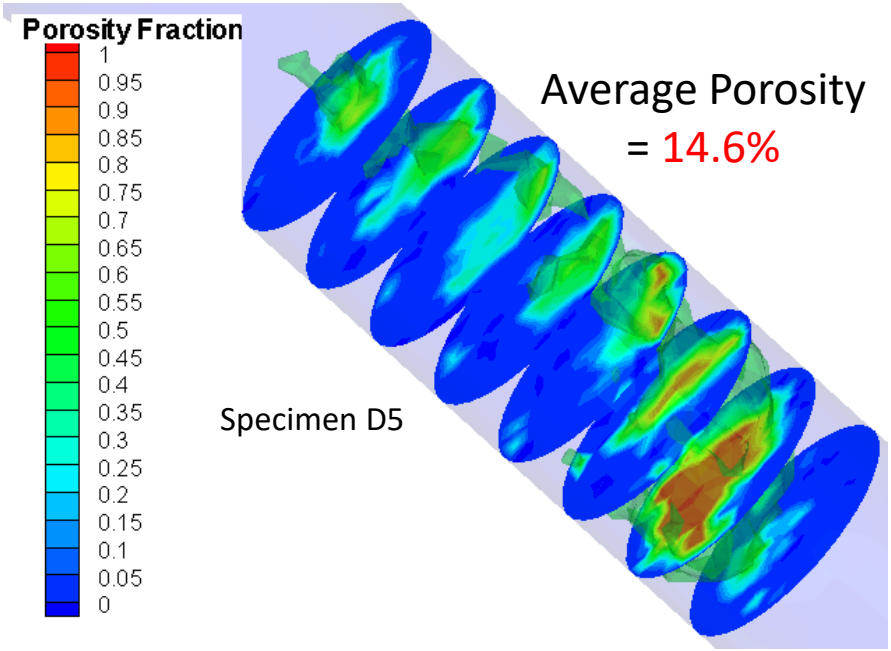


Measured Elastic Modulus = 87 GPa

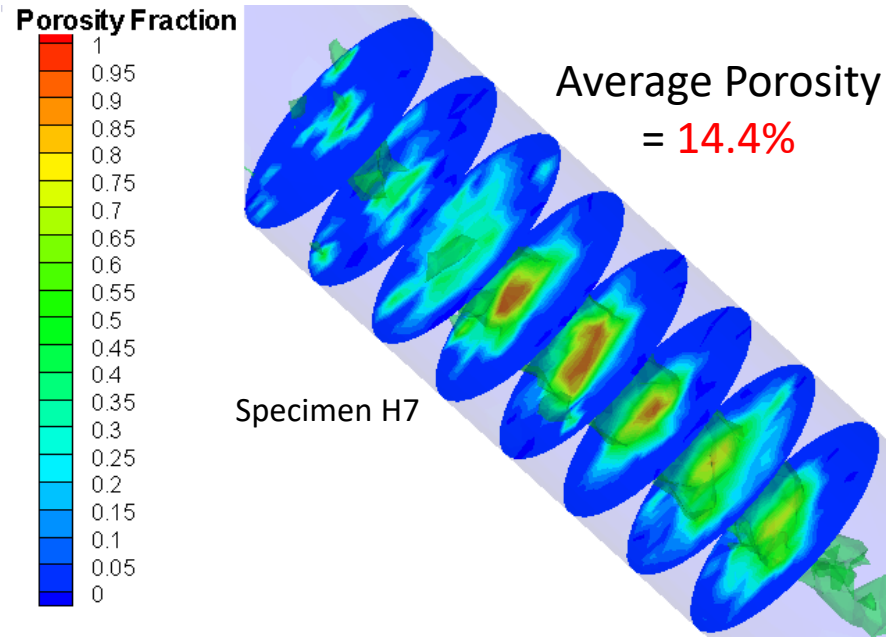


Measured Elastic Modulus = 142 GPa

- Measured elastic moduli differ by about 40%.

# Effect of Porosity on Elastic Behavior: Model Results

FEA predicted strain on surface of test specimen with porosity

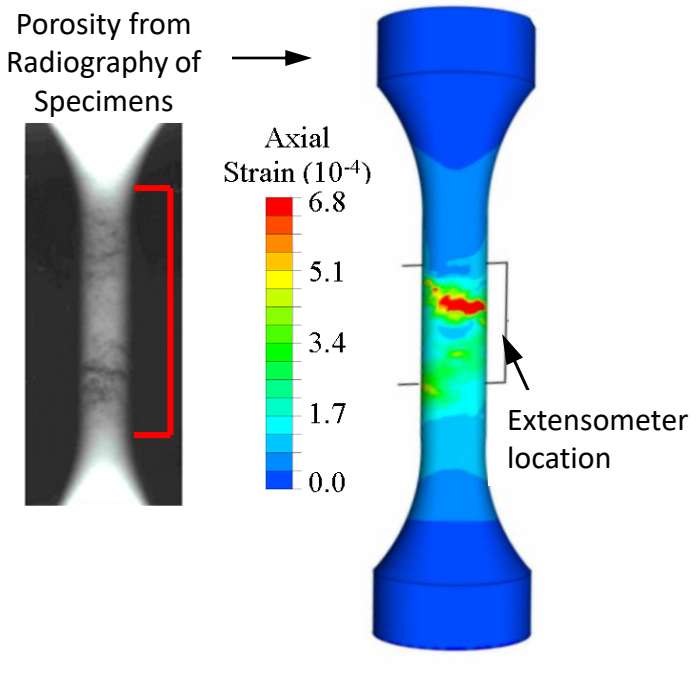


- Porosity causes non-uniform stresses and strains

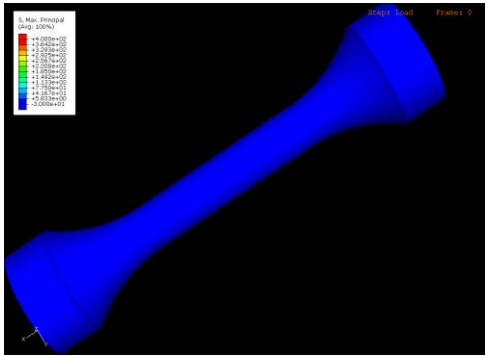

Predicted *vs*. measured strain: FEA uses locally degraded *E* (see formula below) corresponding to measured porosity distribution.

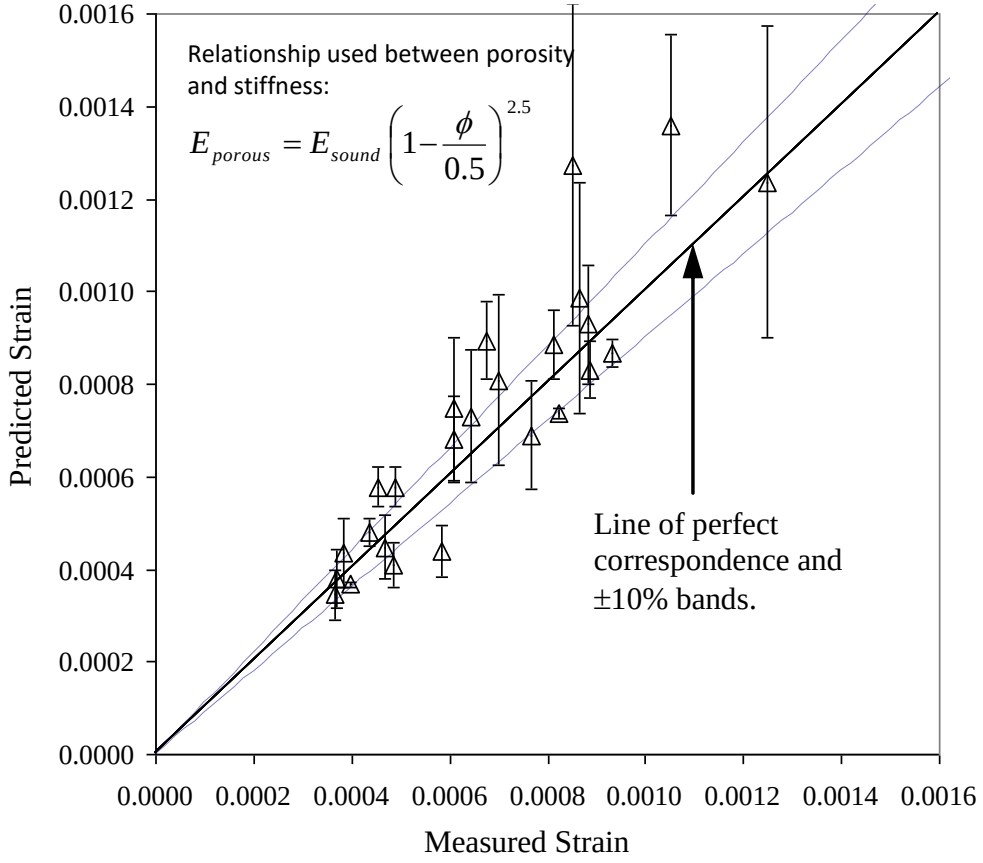


- Relationship between porosity and elastic modulus validated.

# Overview of Fatigue Life Calculations using *fe-safe* from FEA Stresses

1. FEA is performed using locally degraded *E* corresponding to predicted porosity $\phi$.

$$E_{porous} = E_{sound}\left(1-\frac{\phi}{0.5}\right)^{2.5}$$

- FEA performed using elastic-plastic properties and porous metal plasticity failure modeling in ABAQUS. Most steel casting parts are designed to perform in the elastic regime so this is not done here.

2. A pore size model defines maximum pore radius as function of porosity fraction, $\phi$.

3. A local subgrid model, using stress concentration factors $K_t$, is used to correct the FEA stresses to account for un- or under-resolved local stresses at pores.

4. A local fatigue notch factor $K_f$ is calculated as a function of $K_t$, maximum pore radius and material notch sensitivity (Neuber/Peterson).

5. *fe-safe*'s multi-axial Brown-Miller algorithm with critical plane analysis is used to calculate fatigue life using FEA stresses and strain-life fatigue properties ($\sigma_f'$, *b*, $\varepsilon_f'$ and *c*) that are locally degraded according to $K_f$ values.

# Overview of Fatigue Life Calculations using *fe-safe* from FEA Stresses

Step 2: A pore size model defines maximum pore radius as function of porosity fraction, $\phi$.

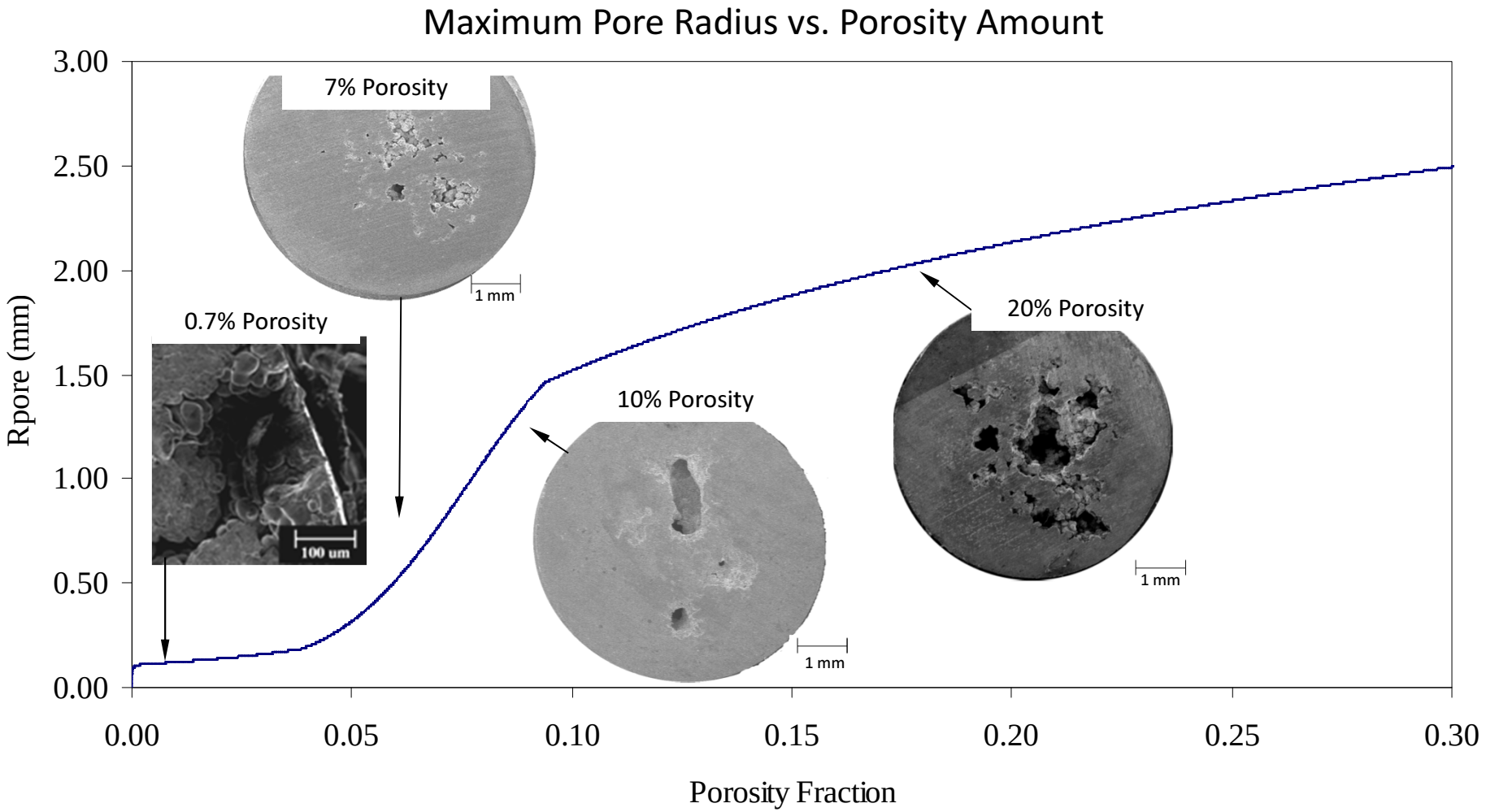


- A probabilistic pore size model and microscopy analysis used to determine maximum pore size as function of pore fraction.

# Overview of Fatigue Life Calculations using *fe-safe* from FEA Stresses

Step 3: Local subgrid model corrects the FEA stresses using a concentration factor for a spherical pore.

- By simulating a spherical hole in a cylindrical specimen a stress concentration factor $K_{t,c}$ needed to achieve the proper local stresses and fatigue life was determined for a range of mesh densities.

Coarse Mesh

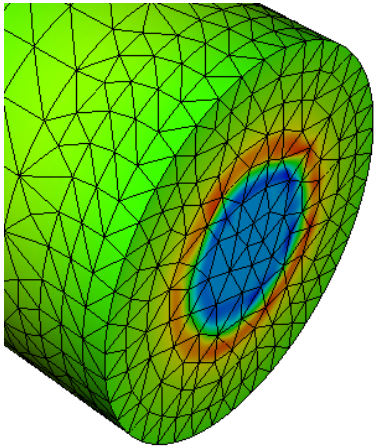

Stress

Mesh is too coarse to give correct maximum stress.

Fine Mesh

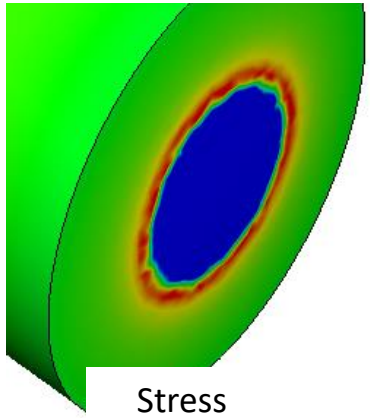


Mesh is fine enough to resolve local stresses.

# Overview of Fatigue Life Calculations using *fe-safe* from FEA Stresses

Step 3: Local subgrid model corrects the FEA stresses assuming porosity is a spherical pore using concentration factor $K_{t,c}$.

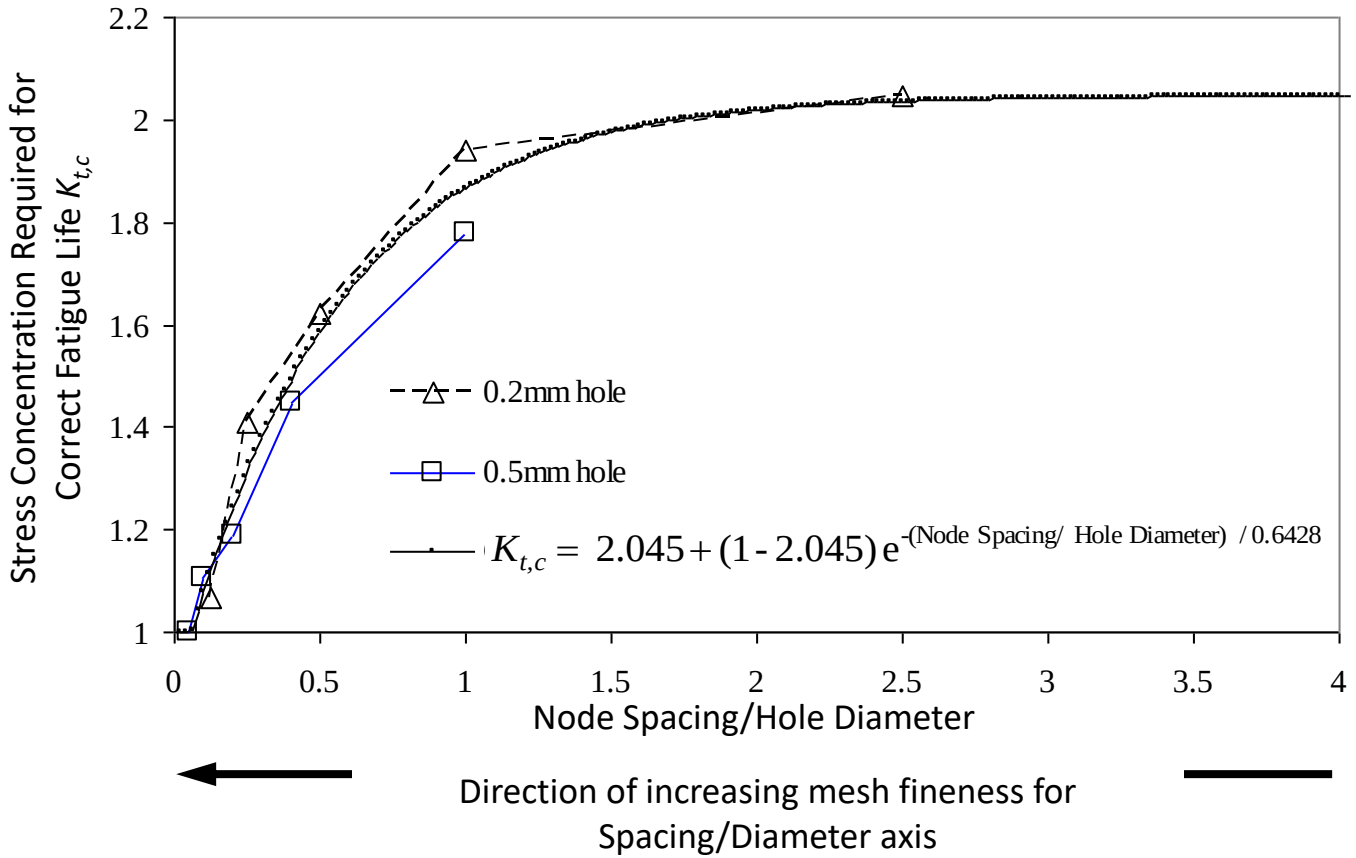


- Maximum $K_{t,c}$ for spherical hole = 2.045

- For fine meshes relative to hole size, FEA stresses are accurate, for coarse meshes stress concentration factor must be applied.

# Overview of Fatigue Life Calculations using *fe-safe* from FEA Stresses

Step 4: Local fatigue notch factor $K_f$ is determined assuming spherical notch of pore radius $R_{pore}$ from Neuber and Peterson relations as function of $K_{t,c}$, $R_{pore}$ and material notch sensitivity $a$ (Neuber/Peterson).

$$K_f = 1 + \frac{K_{t,c} - 1}{1 + a / R_{pore}}$$

where the pore radius $R_{pore}$ is in millimeters, and the material constant $a$ is obtained from the following relation originally developed for wrought steel

$$a = 0.0254 \cdot \left( \frac{2070}{S_u} \right)^{1.8}$$

where $S_u$ is the ultimate strength in MPa.

# Overview of Fatigue Life Calculations using *fe-safe* from FEA Stresses

Step 5: Crack initiation fatigue life is calculated using FEA stresses with *fe-safe*'s multi-axial Brown-Miller algorithm with Morrow mean stress correction and critical plane analysis.

$$\frac{\Delta\gamma_{\max}}{2}+\frac{\Delta\varepsilon_n}{2}=1.65\frac{(\sigma'_f-\sigma_m)}{E}\left(2N_f\right)^b+1.75\varepsilon'_f\left(2N_f\right)^c$$

- The strain-life fatigue properties ($\sigma_f'$, $b$, $\varepsilon_f'$ and $c$) are made functions of $K_f$ at the FEA nodes. For example:

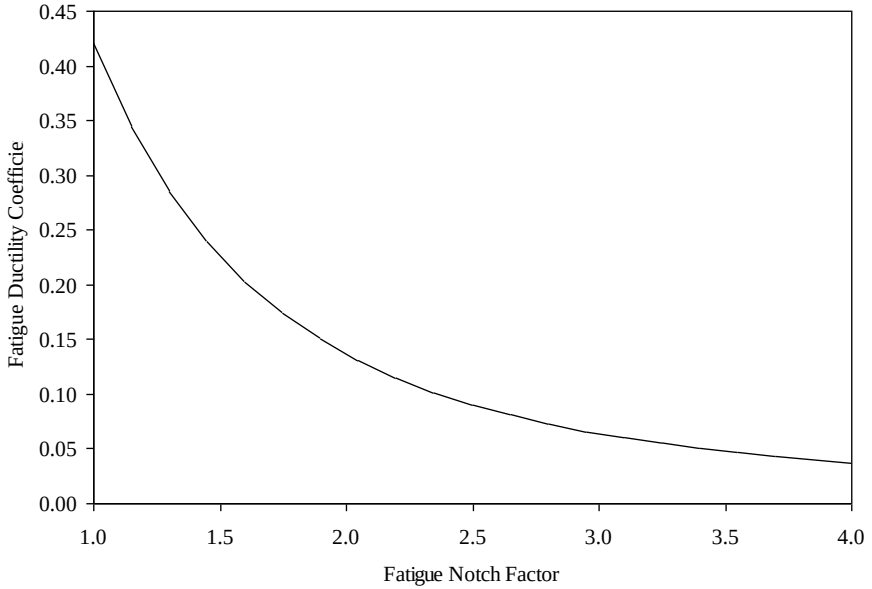

# Fatigue Life Simulation of Test Specimens

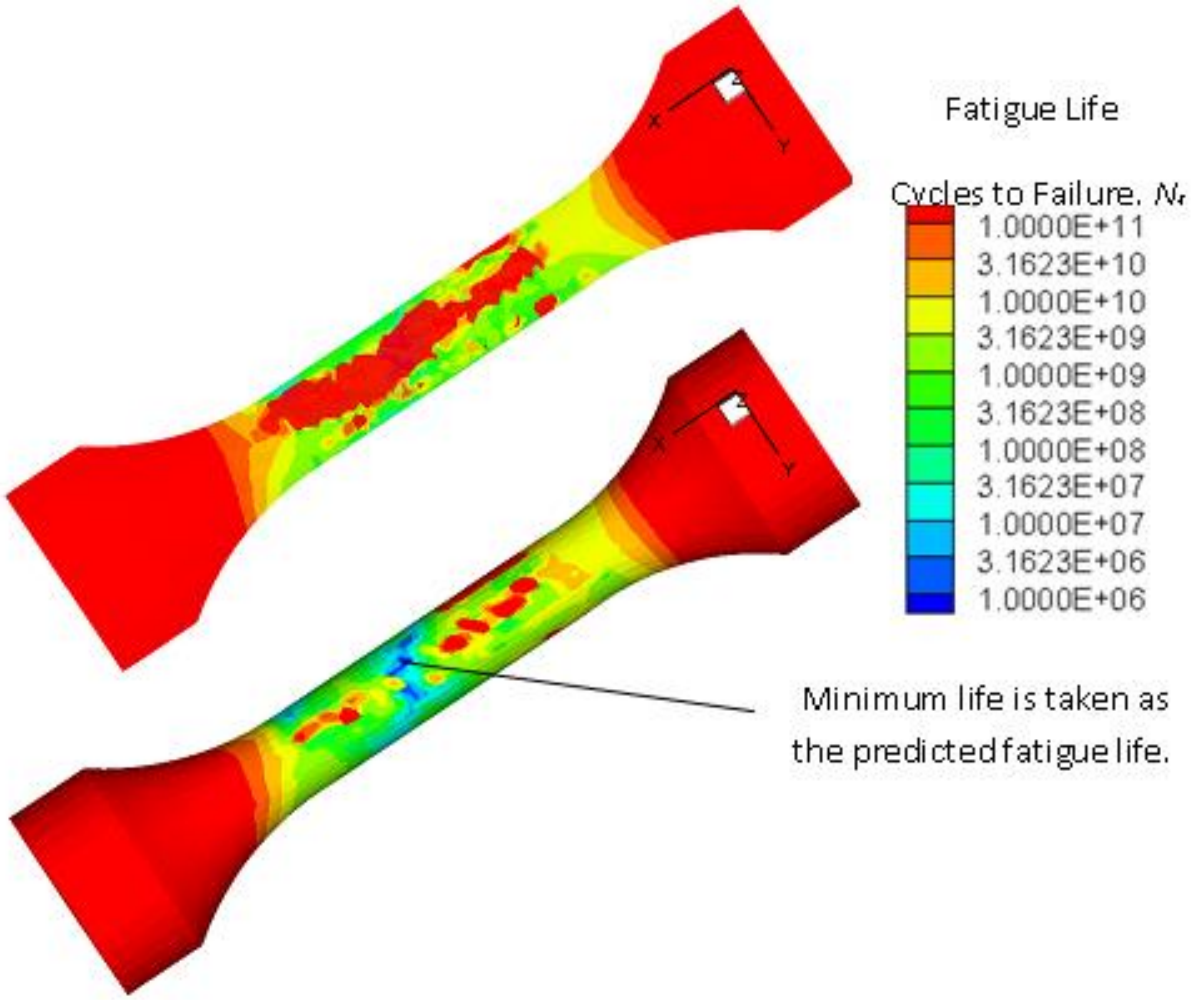

# Effect of Porosity on Fatigue Life

Fatigue Test Specimens with Porosity in Gage Section

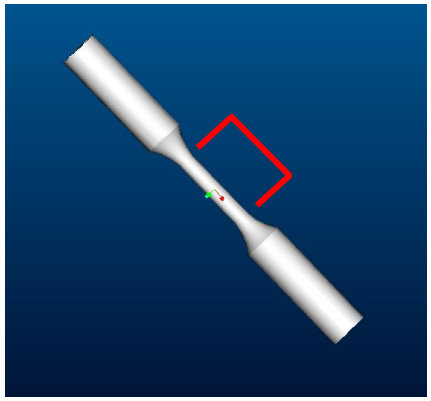

Radiography of Specimens from Orthogonal Views

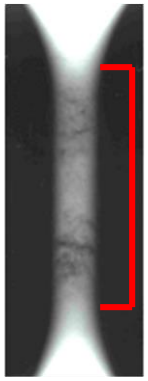

Algebraic Reconstruction of Porosity in Gage Section Performed to Map it to Nodes in ABAQUS FEA Stress Model

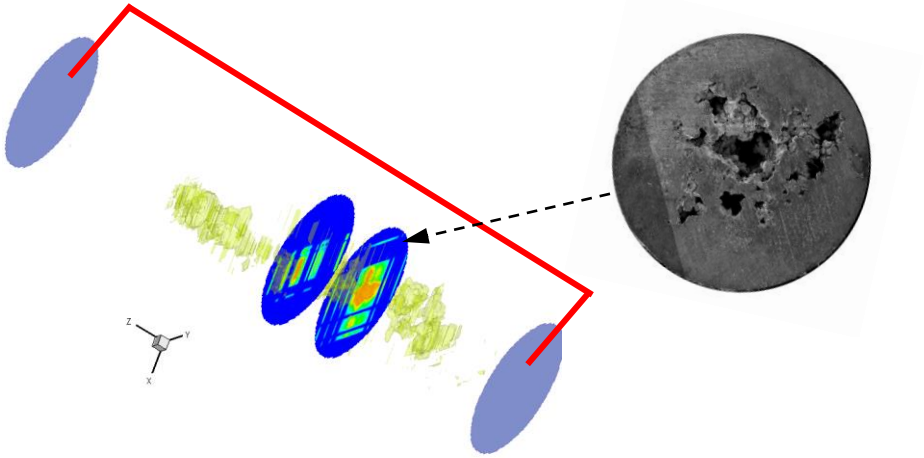

Fatigue Testing Simulated using Material Properties that Depend on Nodal Porosity: Stresses and Fatigue Life Predicted

Simulated Max. Principal Stress during Fatigue Testing

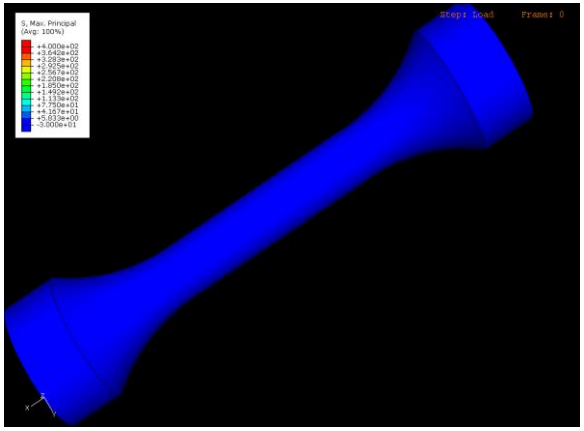

Fatigue Life Prediction

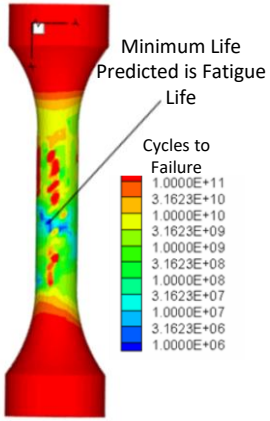


- Multi-axial strain-life fatigue simulations performed using *fe-safe* using stress-strain field from ABAQUS

Comparison of Measured and Predicted Fatigue Life

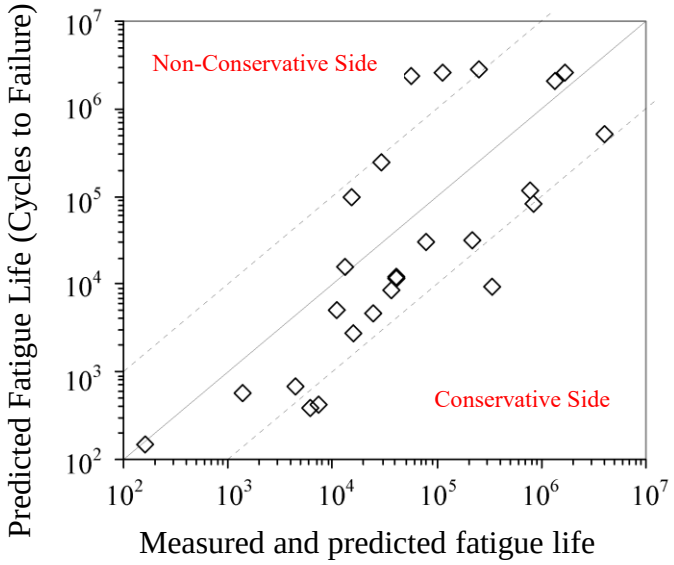

# Steps and Software to link *MAGMAsoft* and FEA Results to Predict Stress/Strain, Fracture and Fatigue Life

Simulate Casting Process and Porosity

**1. MAGMAsoft**

Porosity Results

**2. MAGMAlink Module**

Output from MAGMAlink is nodal values of porosity for use in ABAQUS as a field variable

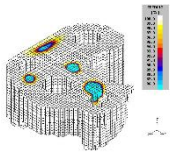

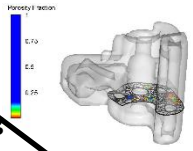

Output from MAGMAlink is post-processed for ABAQUS input

**3. MAGMApost (in-house)**

Generates node set file and nodal porosity field file. Inserted into input deck.

ABAQUS input deck containing mesh nodal data is input to MAGMAlink

**4. ABAQUS**

FEA Model run using elastic-plastic properties as function of porosity field, and porous metal plasticity to predict fracture

ABAQUS Results file with stress and porosity output for load steps defining one cycle

**5. GenNPData (in-house)**

ABAQUS user post-processing code to generate nodal mapped fatigue property data for *fe-safe* and Tecplot compatible visualization files.

Output is fatigue nodal property file and ABAQUS Results file or input into *fe-safe*

**6. fe-safe**

Multiaxial fatigue life prediction using fatigue properties varying node by node as functions of fatigue notch factor

Output is fatigue life at fea nodes, format is ABAQUS Results file.

**7. Postfil (in-house)**

Generates Tecplot compatible visualization files for fatigue life.

**Strain_life_prop_gen (in-house)**

Utility program that generates a table of fatigue property data as functions of fatigue notch factor

**Notes:**

**Commercial software used is white text.**

**Custom in-house software is yellow text.**

# Example: Effect of Porosity on Life of a Cast Control Arm

As-cast Part

Modified Rigging to Induce Porosity in Part*

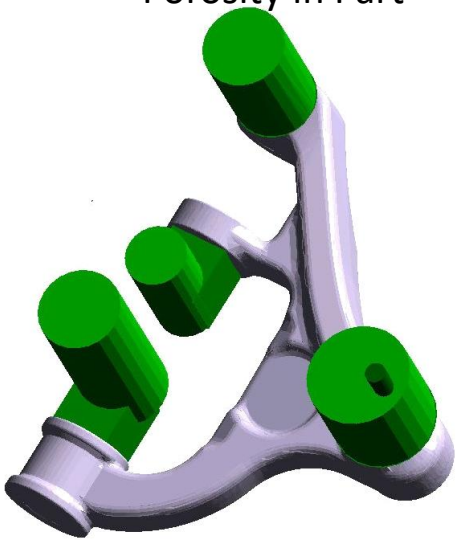

Feeding Indications in Part

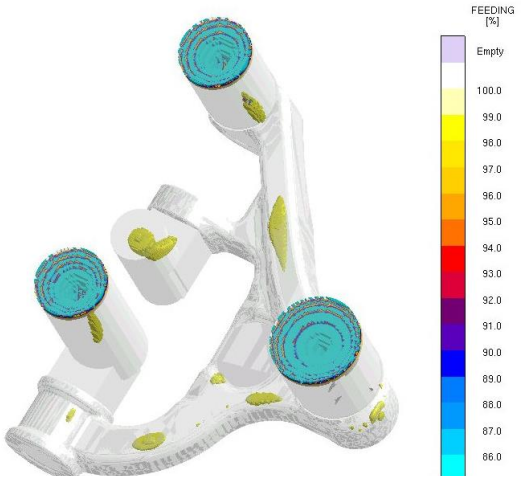


Machined Part and Service Loading Condition for Braking

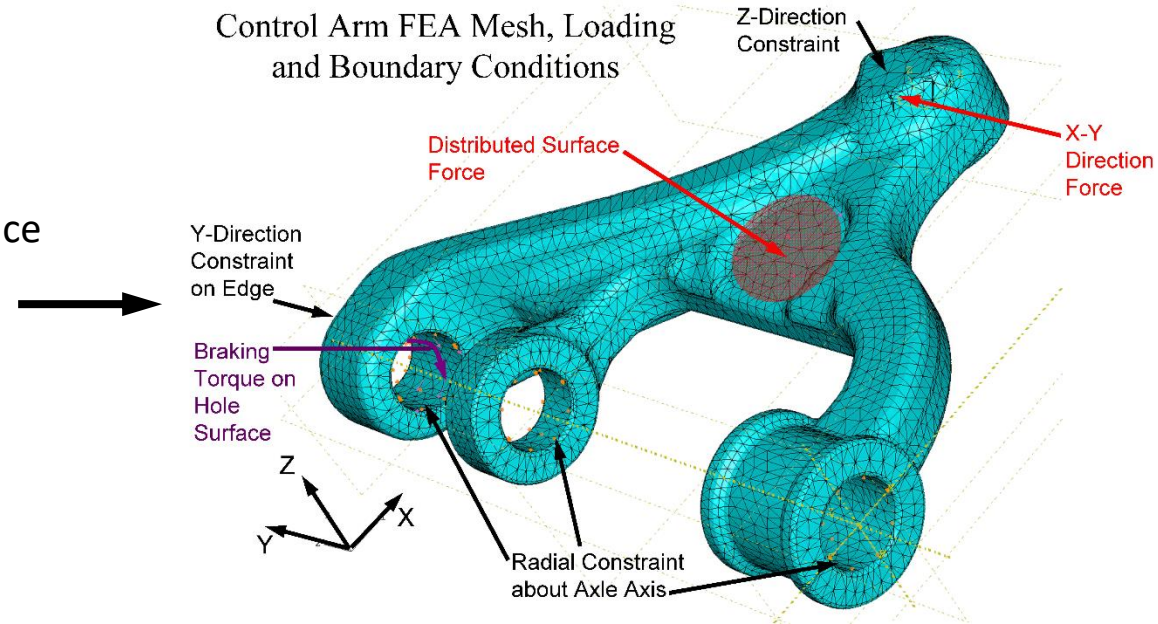

# Control Arm Von Mises Stress and Deflection - Steady and Braking Loads

- Deflection 50x under steady suspension load and during braking shown in animation

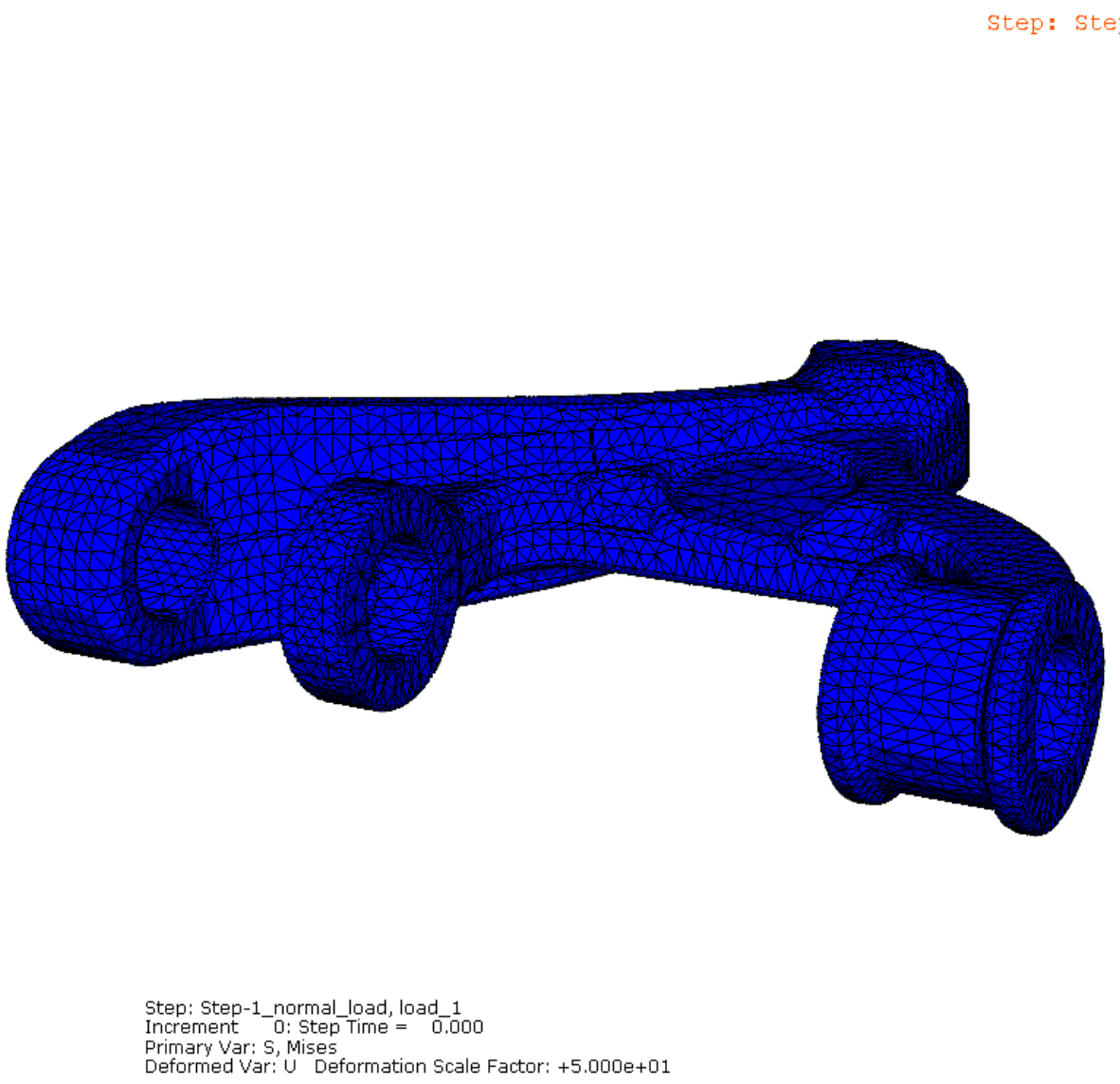

# Porosity and Subgrid Model Notch Factor Results

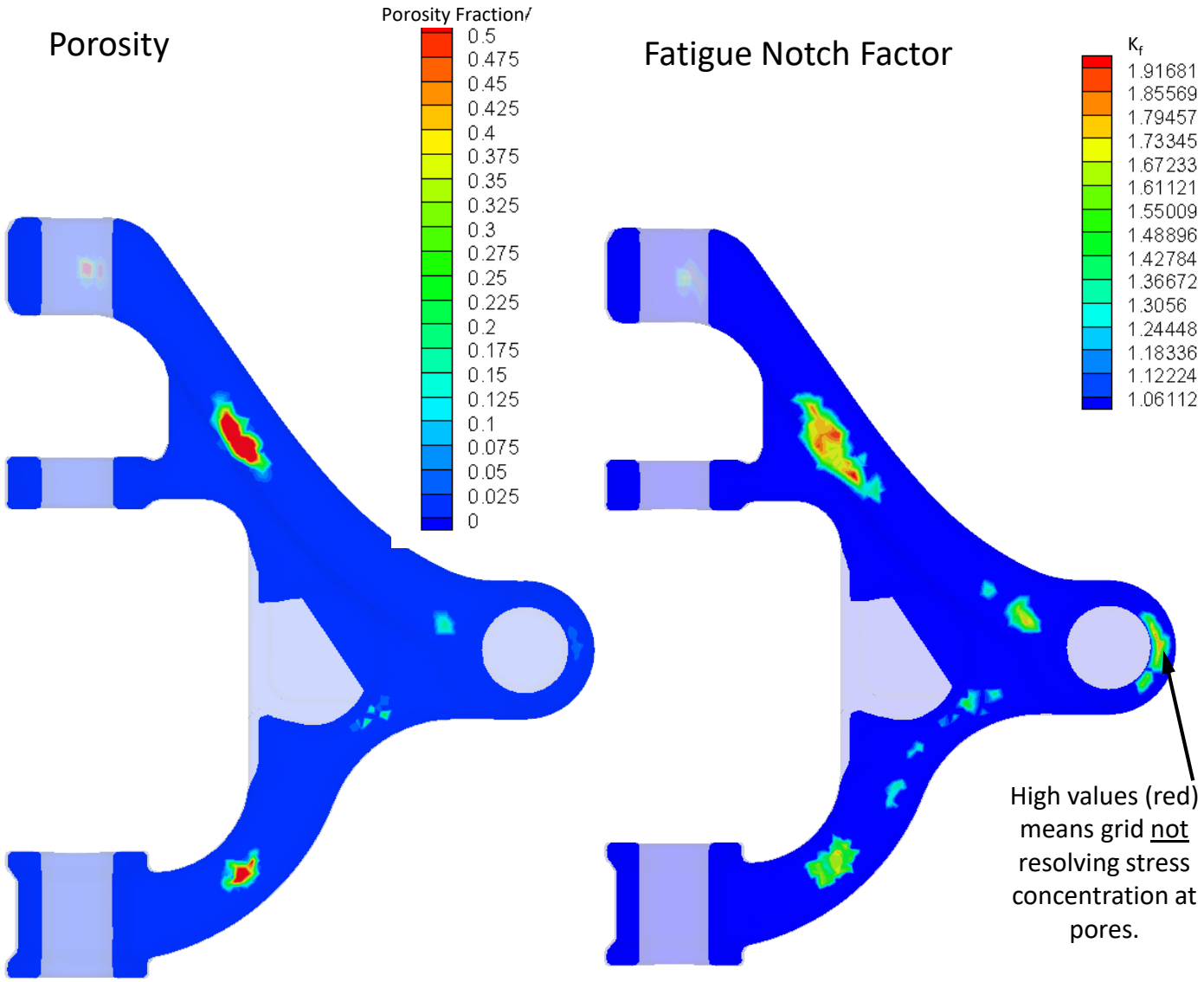

# Control Arm Stress under Steady and Braking Loads

Stresses Under Steady Suspension Load

Without Porosity

With Porosity

Stresses Under Braking Load

Without Porosity

With Porosity

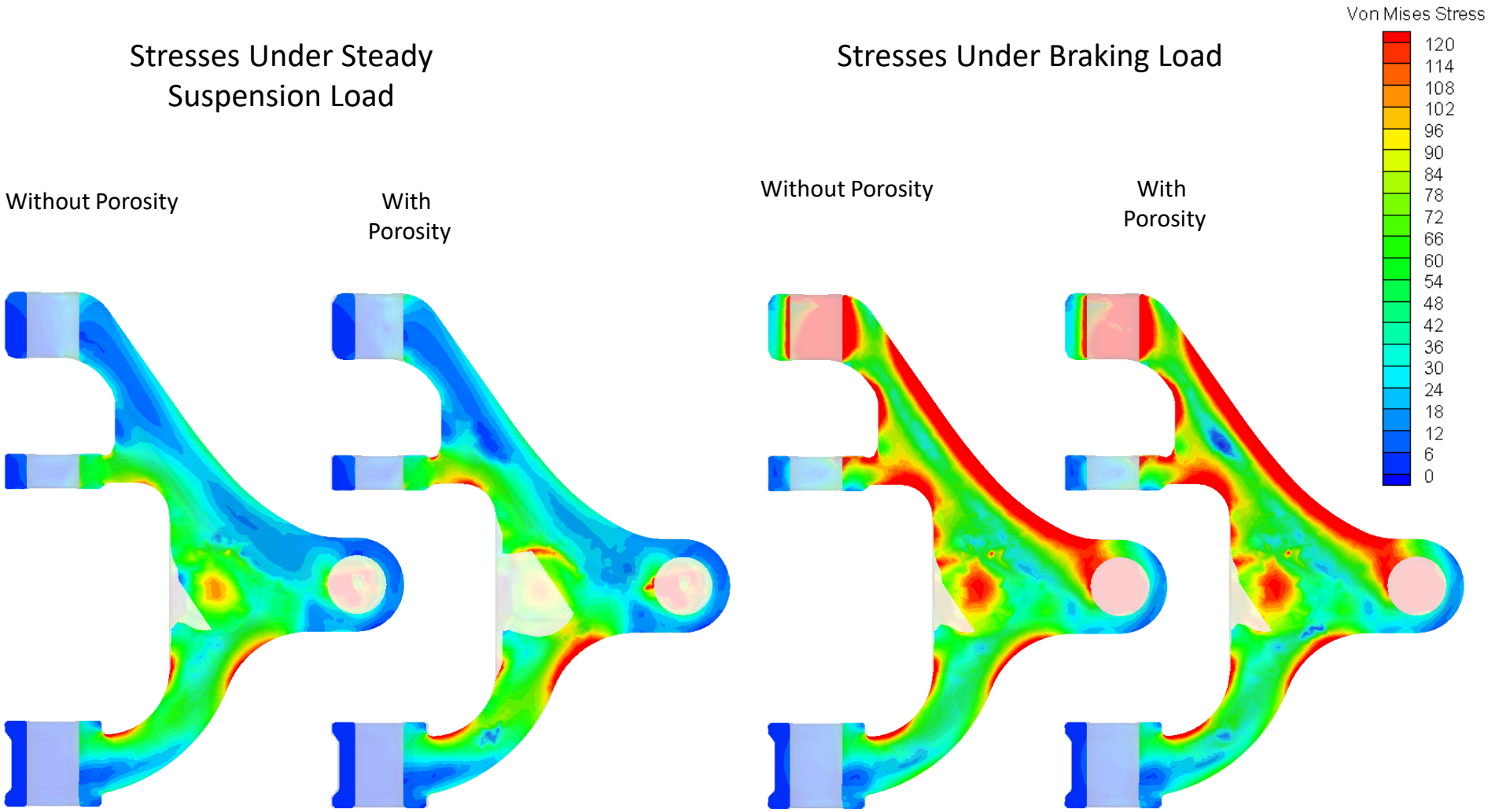


- Stress field from analysis using elastic modulus dependent on porosity to determine stress redistribution.

# Part Stress and Fatigue Life Predictions using *fe-safe*

**Von Mises Stress Results**

Without Porosity

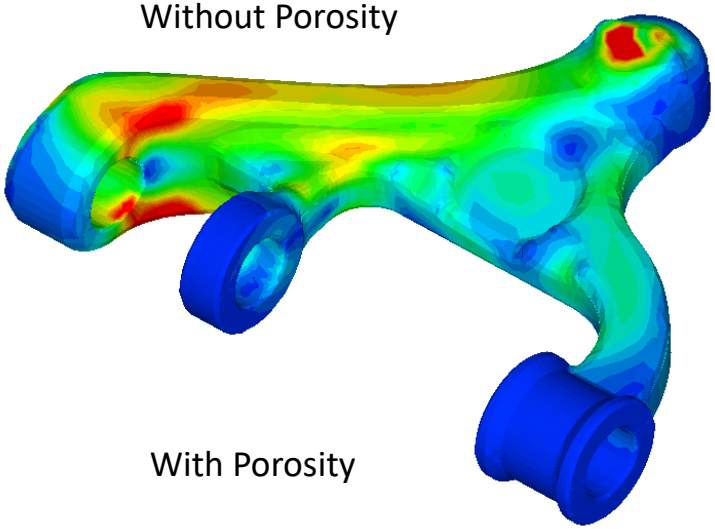

With Porosity

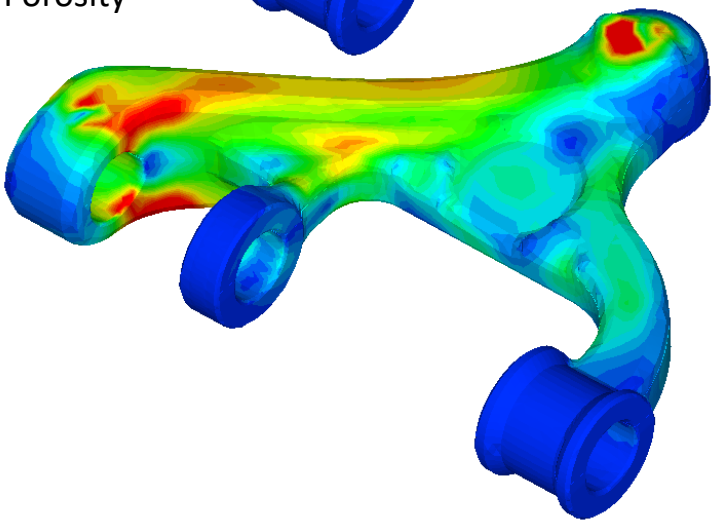

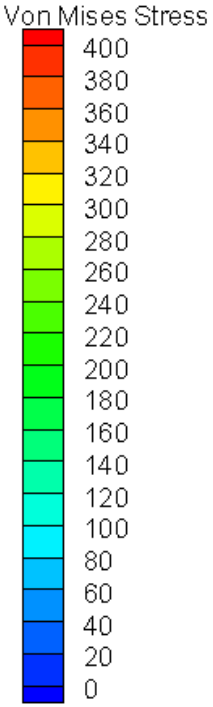


**Fatigue Life Results**

Without Porosity

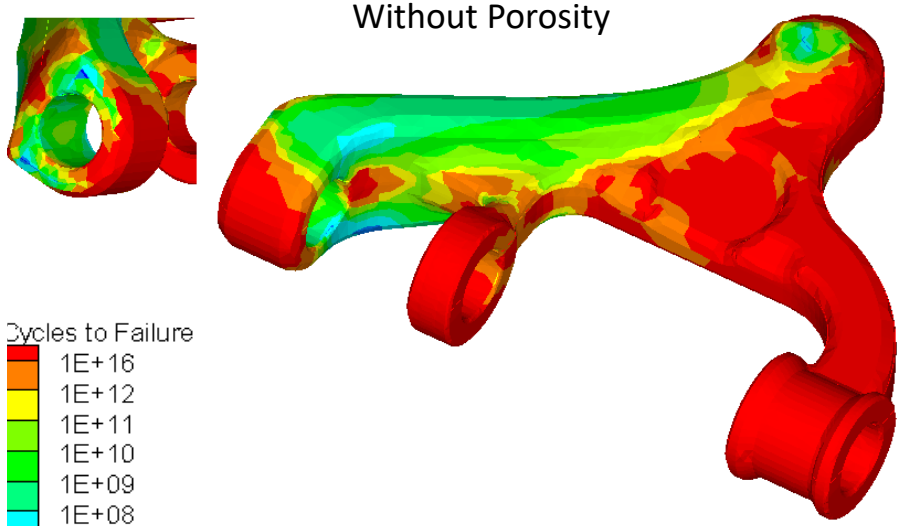




With Porosity

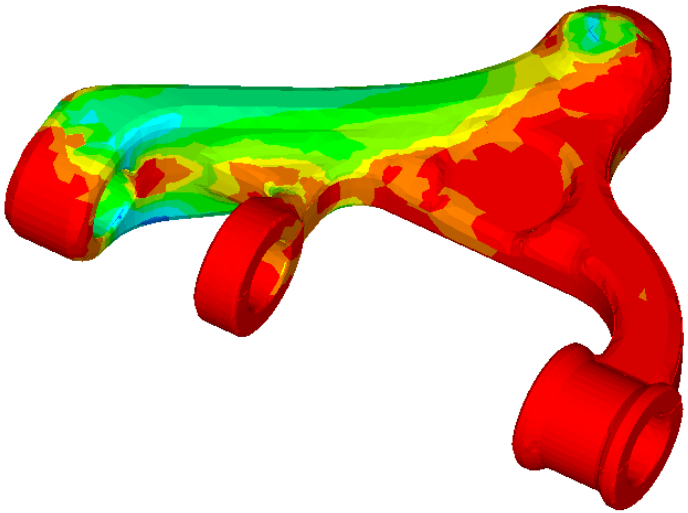

# Bibliography of U Iowa Solidification Lab Research on Fatigue, Porosity, Properties and Steel Performance


- Sigl, K.M., Hardin, R.A., Stephens, R.I., and Beckermann, C., "Fatigue of 8630 Cast Steel in the Presence of Porosity," Int. J. Cast Metals Research, Vol. 17, 2004, pp. 130-146.
- Blair, M., Monroe, R., Beckermann, C., Hardin, R., Carlson, K., and Monroe, C., "Predicting the Occurrence and Effects of Defects in Castings," JOM, Vol. 57, No. 5, 2005, pp. 29-34.
- Deegan, P.T., Stephens, R.I., Hardin, R.A., and Beckermann, C., "The Effect of Porosity on the Fatigue Life of 8630 Cast Steel," AFS Transactions, Vol. 115, Paper No. 07-120, 2007, pp. 787-803.
- Hardin, R.A., and Beckermann, C., "Effect of Porosity on the Stiffness of Cast Steel," Metall. Mater. Trans. A, Vol. 38A, 2007, pp. 2992-3006.
- Hardin, R.A., and Beckermann, C., "Prediction of the Fatigue Life of Cast Steel Containing Shrinkage Porosity," Metall. Mater. Trans. A, Vol. 40A, 2009, pp. 581-597.
- Hardin, R.A., and Beckermann, C., "Integrated Design of Steel Castings: Case Studies," in Proceedings of the 63rd SFSA Technical and Operating Conference, Paper No. 2.3, Steel Founders' Society of America, Chicago, IL, 2009.
- Hardin, R.A., and Beckermann, C., "Effect of Porosity on Deformation, Damage, and Fracture of Cast Steel," Metall. Mater. Trans. A, Vol. 44A, 2013, pp. 5316-5332.
- Hardin, R.A., and Beckermann, C., "Effect of Cooling Rate and Microporosity on Mechanical Performance of a High Strength Steel," in Proceedings of the 70th SFSA Technical and Operating Conference, Paper No. 5.2, Steel Founders' Society of America, Chicago, IL, 2016.
- Weidt, M., Hardin, R.A., Garb, C., Rosc, J., Brunner, R., and Beckermann, C., "Prediction of Porosity Characteristics of Aluminium Castings Based on X-ray CT Measurements," Int. J. Cast Metals Research, Vol. 31, 2018, pp. 289-307.
- Ardis, A., Harper, P., Hardin, R., Beckermann, C., Griffin, J., Foley, R., Monroe, C., Poweleit, D., David, D., and Lynch, P., "Mechanical Properties of Test Bars and Castings Sections and an Analysis of the Cost of Equivalent Round Test Bars," in Proceedings of the 73rd SFSA Technical and Operating Conference, Paper No. 3.10, Steel Founders' Society of America, Chicago, IL, 2019.
- Hardin, R., Beckermann, C., Monroe, R., David, D., and Allyn, B., "Measurements and Predictions of Lower Bound Mechanical Properties of Cast Steels," in Proceedings of the 73rd SFSA Technical and Operating Conference, Paper No. 4.3, Steel Founders' Society of America, Chicago, IL, 2019.
- Poweleit, D., Brown, H., David, D., Hardin, R., Beckermann, C., Foley, R., and Griffin, J., "Establishing Lower Bound Properties for Cast Parts," in Proceedings of the 74th SFSA Technical and Operating Conference, Steel Founders' Society of America, Chicago, IL, 2020.